
On the Expressiveness of Approximate Inference in Bayesian Neural Networks

Andrew Y. K. Foong^{*1} David R. Burt^{*1} Yingzhen Li² Richard E. Turner^{1,2}

Abstract

While Bayesian neural networks (BNNs) hold the promise of being flexible, well-calibrated statistical models, inference often requires poorly understood approximations. We study the impact of approximate inference in BNNs on the quality of uncertainty quantification, focusing on methods that use parametric approximating distributions. For single-hidden layer ReLU BNNs, we prove a fundamental limitation in *function-space* of two of the most ubiquitous distributions defined in *weight-space*: mean-field Gaussian and Monte Carlo dropout. In particular, neither method can have substantially increased uncertainty in between well-separated regions of low uncertainty. In contrast, for deep networks, we prove a universality result showing that there exist distributions in the above classes which provide flexible uncertainty estimates. However, we find that *in practice* pathologies of the same form as in the single-hidden layer case often persist when performing variational inference in deeper networks. Our results motivate careful consideration of the implications of approximate inference methods in BNNs.

1. Introduction

Bayesian neural networks (BNNs) (MacKay, 1992; Neal, 1995) aim to combine the strong inductive biases and flexibility of neural networks (NNs) with the probabilistic framework for uncertainty quantification provided by Bayesian statistics. BNNs are applied in many domains where quantifying uncertainty is critical to success. For example, they have been proposed for use in medical applications, where predictive uncertainty is used to determine which patients should be referred to an expert (Filos et al., 2019). In reinforcement learning, Bayesian optimisation and active learn-

ing, model uncertainty can be used to promote exploration (Deisenroth & Rasmussen, 2011; Springenberg et al., 2016; Gal et al., 2017).

Unfortunately, performing exact inference in BNNs is analytically intractable and requires approximations. Therefore, the efficacy of the resulting predictions depends not only on the suitability of the modelling assumptions, but also on the quality of approximate inference. A variety of scalable approximate inference techniques have been proposed, with mean-field variational inference (MFVI) (Hinton & Van Camp, 1993; Blundell et al., 2015) and Monte Carlo dropout (MCDO), which has also been interpreted as variational inference (Gal & Ghahramani, 2016), among the most popular methods. Recently, MFVI has been applied to large-scale classification tasks (Osawa et al., 2019). However, BNNs have yet to become mainstream in deep learning, in part due to concerns raised regarding the quality of the uncertainty estimates obtained by these methods (Springenberg et al., 2016; Ovadia et al., 2019; Osband, 2016; Fort et al., 2019). Hence it is crucial to ask, *what do we lose by performing approximate inference?* Answering this will not only identify limitations of our methods, but will also help us understand to what extent the *successes* of approximate BNNs are attributable to Bayesian principles.

Frequently, BNN approximations involve defining a simple class of distributions over the model parameters, (which we refer to as an *approximating family*), and then choosing a member of this family as an approximation to the posterior. Both MFVI and MCDO follow this paradigm. In order for such a method to be successful, two criteria must be met:

Criterion 1 The approximating family must be sufficiently expressive to contain good approximations to the posterior.

Criterion 2 The method must then select a good approximate posterior within this family.

For nearly all tasks, the performance of a BNN only depends on the distribution over weights to the extent that it affects the distribution over network outputs (i.e. in ‘function-space’). Hence for our purposes, a ‘good’ approximation is one that captures features of the exact posterior in function-space that are relevant to the task at hand. However, approximating families are often defined in weight-space for computational reasons. Evaluating **Criterion 1** therefore involves understanding how weight-space approximations

^{*}Equal contribution ¹University of Cambridge, Cambridge, UK ²Microsoft Research, Cambridge, UK. Correspondence to: Andrew Y. K. Foong <ykf21@cam.ac.uk>, David R. Burt <drb62@cam.ac.uk>.

translate to function-space.

We present an extensive study on the quality of approximate inference in BNNs using mean-field Gaussian and MC dropout approximations. Specifically, we provide theoretical and empirical analyses of the flexibility of the approximate predictive mean and variance functions of BNNs. Our major findings are:

1. For shallow BNNs, neither mean-field Gaussian nor MC dropout distributions are capable of expressing meaningful uncertainty in many situations, thus failing Criterion 1.

We prove in section 3 the surprising result that the variance function of any fully-connected, single-hidden layer ReLU BNN using these families necessarily suffers from a lack of ‘*in-between uncertainty*’: increased uncertainty in between well-separated regions of low uncertainty. We show that the exact posterior does not have this limitation; hence this pathology is attributable solely to the restrictiveness of the approximating family.

2. For deeper BNNs, both the mean-field Gaussian and MC dropout families are sufficiently flexible in theory, but in practice the variational inference (VI) algorithm for selecting the approximate posterior often fails to return satisfactory uncertainty estimates, thus failing Criterion 2.

In section 4 we prove a universal approximation result showing that the mean and variance functions of deep BNNs using mean-field Gaussian or MCDO distributions can approximate any continuous function and any continuous non-negative function respectively. Therefore **Criterion 1** is satisfied for tasks which mainly depend on the first two moments of the predictive distribution, such as common algorithms for Bayesian optimisation, active learning and expert referral. However, we provide empirical evidence that in spite of this flexibility, VI in deep BNNs leads to distributions that suffer from similar pathologies to the shallow case, i.e. **Criterion 2** is not satisfied.

We demonstrate in section 5 the practical impact of poorly calibrated in-between uncertainty, with a case study on active learning on a real-world dataset. We show that although the inductive biases of the BNN model can bring considerable benefits in this task, these are lost when MFVI or MCDO are used.

2. Background

We focus on BNN regression. The goal is to model our beliefs concerning which functions could plausibly have generated the data, and use these to make predictions.

2.1. Bayesian Neural Networks

Consider a regression dataset $\mathcal{D} = \{(\mathbf{x}_n, y_n)\}_{n=1}^N$ with $\mathbf{x}_n \in \mathbb{R}^D$ and $y_n \in \mathbb{R}$. To define a BNN, we first specify a prior distribution with density $p(\theta)$ over the

NN parameters. Each parameter setting corresponds to a function $f_\theta : \mathbb{R}^D \rightarrow \mathbb{R}$. Although the prior is defined over parameters, the distribution over functions is the true object of interest. We next specify a likelihood $p(\{y_n\}_{n=1}^N | \{\mathbf{x}_n\}_{n=1}^N, f_\theta)$ which describes the relationship between the observed data and the model parameters. The posterior distribution over parameters then has density $p(\theta | \mathcal{D}) \propto p(\{y_n\}_{n=1}^N | \{\mathbf{x}_n\}_{n=1}^N, f_\theta) p(\theta)$. The posterior does not have a closed form and approximations must be made in order to make predictions.

2.2. Approximate Inference Methods

Many approximate inference methods begin by defining a class of distributions \mathcal{Q} where each distribution in \mathcal{Q} is parameterised by a vector ϕ . We refer to \mathcal{Q} as the *approximating family*, and such methods as *approximating family methods*. For BNNs, the distributions in \mathcal{Q} are defined over the model parameters θ . For example, \mathcal{Q} might consist of fully-factorised Gaussian distributions, in which case ϕ is a vector of means and variances. We denote this fully-factorised Gaussian family as \mathcal{Q}_{FFG} .

Given the approximating family \mathcal{Q} , these methods aim to select a distribution $q_\phi(\theta) \in \mathcal{Q}$ that best approximates the exact posterior according to some criteria. Once q_ϕ is selected¹, predictions at a test point (\mathbf{x}_*, y_*) can be made by replacing the expectation under the exact posterior by an expectation under the approximate posterior:

$$\begin{aligned} p(y_* | \mathbf{x}_*, \mathcal{D}) &= \mathbb{E}_{p(\theta | \mathcal{D})} [p(y_* | \mathbf{x}_*, f_\theta)] \approx \mathbb{E}_{q_\phi(\theta)} [p(y_* | \mathbf{x}_*, f_\theta)] \\ &\approx \frac{1}{M} \sum_{m=1}^M p(y_* | \mathbf{x}_*, f_{\theta_m}), \end{aligned} \quad (1)$$

where $\theta_m \sim q_\phi$ in equation (1). Various approximating family methods may share the same \mathcal{Q} , e.g. VI, the diagonal Laplace approximation (Denker & Lecun, 1991), probabilistic backpropagation (Hernández-Lobato & Adams, 2015), stochastic expectation propagation (Li et al., 2015), black-box alpha divergence minimisation (Hernández-Lobato et al., 2016), Rényi divergence VI (Li & Turner, 2016), natural gradient VI (Khan et al., 2018) and functional variational BNNs (Sun et al., 2019) all frequently use \mathcal{Q}_{FFG} .

Variational Inference VI (Beal, 2003; Jordan et al., 1999) is an approximating family method that minimises the KL divergence between the approximate and exact posterior to choose q_ϕ (Blei et al., 2017). This is equivalent to maximising an evidence lower bound (ELBO):

$$\mathcal{L}(\phi) = \sum_{n=1}^N \mathbb{E}_{q_\phi} [\log p(y_n | \mathbf{x}_n, f_\theta)] - \text{KL} [q_\phi(\theta) || p(\theta)],$$

¹We often suppress the θ -dependence in both f_θ and $q_\phi(\theta)$.

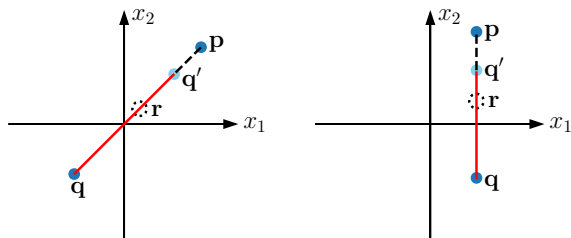


Figure 1. Illustration of the bounded regions in theorem 1, showing the input domain of a 1HL mean-field Gaussian BNN, for the case $\mathbf{x} \in \mathbb{R}^2$. Left (resp. Right): For any two points \mathbf{p} and \mathbf{q} such that the line joining them crosses the origin (resp. is orthogonal to and intersects a plane $x_d = 0$), the output variance at any point \mathbf{r} on the solid red portion of the line is upper bounded by $\mathbb{V}[f(\mathbf{p})] + \mathbb{V}[f(\mathbf{q})]$, illustrating condition (i) (resp. condition (ii)) of theorem 1. The bounded region extends from $\mathbf{q} = (q_1, q_2)$ to \mathbf{q}' , where $\mathbf{q}' = (-q_1, -q_2)$ (Left), or $\mathbf{q}' = (q_1, -q_2)$ (Right).

which can be optimised with gradient-based methods. The most commonly used family for VI with BNNs is \mathcal{Q}_{FFG} . This is known as mean-field variational inference.

Monte Carlo Dropout MCDO is another highly scalable approximating family method that works by training a NN with dropout (Srivastava et al., 2014), and averaging multiple stochastic forward passes to make predictions. MCDO has a Bayesian interpretation (Gal, 2016; Hron et al., 2018), in which the stochasticity is viewed as occurring in weight space. This corresponds to randomly setting columns of the weight matrices to zero. Gal (2016) argued that dropout training with ℓ_2 regularisation approximates VI. The variational family, $\mathcal{Q}_{\text{MCDO}}$, is the set of distributions over weight matrices with the sampling procedure $\widehat{\mathbf{W}} := \mathbf{W}\text{diag}(\epsilon)$ where each element of ϵ is Bernoulli distributed with parameter $1 - p$, where p is the dropout probability. The variational parameters ϕ are the pre-dropout weight matrices \mathbf{W} and the biases. Applying dropout at test time is viewed as approximate marginalisation (equation (1)). Frequently, the first weight matrix \mathbf{W}_1 is taken to be deterministic (i.e. inputs are not dropped out) — we analyse this case in the main body and use $\mathcal{Q}_{\text{MCDO}}$ to refer to this family. There are fundamentally different considerations when \mathbf{W}_1 is also stochastic, addressed in appendix D.

3. Single-Hidden Layer Networks

In this section, we prove that for single-hidden layer (1HL) ReLU BNNs, \mathcal{Q}_{FFG} and $\mathcal{Q}_{\text{MCDO}}$ are not expressive enough to satisfy **Criterion 1**. We identify structural constraints on the variance in function-space, $\mathbb{V}[f(\mathbf{x})]$, implied by these families. We show empirically that the exact posterior does

not have these restrictions, implying that approximate inference does not even qualitatively resemble the posterior.

Theorem 1 (Factorised Gaussian). *Consider any single-hidden layer fully-connected ReLU NN $f : \mathbb{R}^D \rightarrow \mathbb{R}$. Let x_d denote the d^{th} element of the input vector \mathbf{x} . Suppose we have a fully factorised Gaussian distribution over the weights and biases in the network. Consider any points $\mathbf{p}, \mathbf{q}, \mathbf{r} \in \mathbb{R}^D$ such that $\mathbf{r} \in \overrightarrow{\mathbf{p}\mathbf{q}}$ and either:*

- i. $\overrightarrow{\mathbf{p}\mathbf{q}}$ contains $\mathbf{0}$ and \mathbf{r} is closer to $\mathbf{0}$ than both \mathbf{p} and \mathbf{q} .
- ii. $\overrightarrow{\mathbf{p}\mathbf{q}}$ is orthogonal to and intersects the plane $x_d = 0$, and \mathbf{r} is closer to the plane $x_d = 0$ than both \mathbf{p} and \mathbf{q} .

Then $\mathbb{V}[f(\mathbf{r})] \leq \mathbb{V}[f(\mathbf{p})] + \mathbb{V}[f(\mathbf{q})]$.

Remark 1. *Conditions i., ii. are illustrated in figure 1. A more general version of theorem 1, which allows for correlations between certain weights, and applies to multi-output BNNs is stated and proved in appendix A.*

Theorem 1 states that there are line segments in input space such that the predictive variance on the line is bounded in terms of the variance at the endpoints. Analogous bounds on higher dimensional sets in input space enclosed by these lines can be obtained as a corollary (see appendix A). Theorem 1 applies to any method using \mathcal{Q}_{FFG} , as listed in section 2.2.

Theorem 2 (MC dropout). *Consider the same network architecture as in theorem 1. Suppose we have an MC dropout distribution over the parameters in the network, such that inputs are not dropped out. Then $\mathbb{V}[f(\mathbf{x})]$ is convex in \mathbf{x} .*

Remark 2. *A more general version of theorem 2 that applies to multi-output BNNs is stated and proved in appendix A. In the case where input dimensions are dropped out, we prove the variance at the origin is bounded by the maximum of the variance at any collection of points S such that the convex hull of S contains the origin. See appendix D for details. This result also applies to variational Gaussian dropout (Kingma et al., 2015).*

Theorem 2 upper bounds the predictive variance on any line in input space by the variance at the endpoints. Theorems 1 and 2 indicate that 1HL approximate BNNs using \mathcal{Q}_{FFG} and $\mathcal{Q}_{\text{MCDO}}$ struggle to represent *in-between uncertainty*: i.e. increased uncertainty in between well separated regions of low uncertainty. As theorems 1 and 2 depend only on the approximating family, this cannot be fixed by improving the optimiser, regulariser or prior. Figure 2 shows a numerical verification of theorems 1 and 2. We train 1HL networks of width 50 with \mathcal{Q}_{FFG} and $\mathcal{Q}_{\text{MCDO}}$ distributions to minimise the squared error between $\mathbb{V}[f(x)]$ and a target variance function displaying in-between uncertainty. We use gradient descent with the reparameterisation trick (Kingma & Welling, 2014) on a Monte Carlo estimate of the predictive variance to perform the optimisation. Full details are given in appendix E.

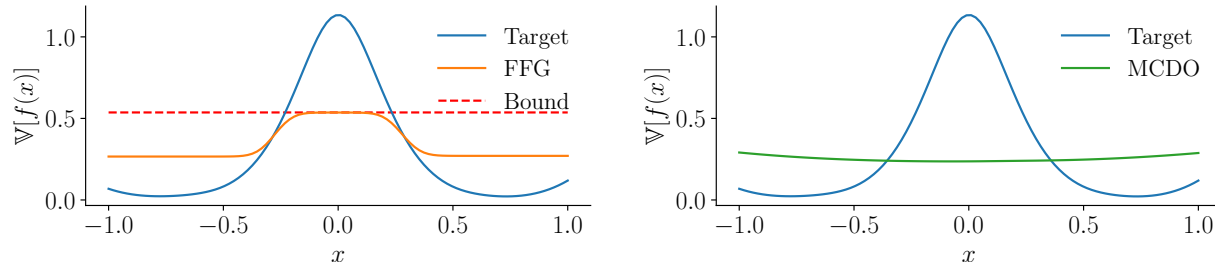


Figure 2. Results of directly minimising the squared error in function space between $\mathbb{V}[f(x)]$ (for a single-hidden layer NN) and a target variance function. Left: FFG distribution, Right: MCDO distribution. The bound for FFG distributions (red) applies on $[-1, 1]$ with $\mathbf{p} = -1, \mathbf{q} = 1$. The MCDO variance function is convex, and almost constant. Note that the FFG and MCDO variance functions underestimate the target near the origin and overestimate it away from the origin.

3.1. Intuition for Theorems 1 and 2

We now provide intuition for the proofs of theorems 1 and 2. Let the weight matrix and bias vector in the first linear layer be collectively denoted θ_{in} . Applying the law of total variance:

$$\mathbb{V}[f(\mathbf{x})] = \mathbb{E}[\mathbb{V}[f(\mathbf{x})|\theta_{\text{in}}]] + \mathbb{V}[\mathbb{E}[f(\mathbf{x})|\theta_{\text{in}}]]. \quad (2)$$

In the case of $\mathcal{Q}_{\text{MCDO}}$ the second term is 0 as θ_{in} is deterministic. To prove theorem 2, it suffices to show the first term is convex. Expanding the first term:

$$\begin{aligned} \mathbb{V}[f(\mathbf{x})|\theta_{\text{in}}] &= \mathbb{V}\left[\sum_{i=1}^I w_i \psi(a_i(\mathbf{x}; \theta_{\text{in}})) + b \mid \theta_{\text{in}}\right] \\ &= \sum_{i=1}^I \mathbb{V}[w_i \psi(a_i(\mathbf{x}; \theta_{\text{in}}))^2] + \mathbb{V}[b], \end{aligned} \quad (3)$$

where $\{w_i\}_{i=1}^I$ and b are the output weights and bias, $\psi(\cdot)$ is the ReLU non-linearity, and $a_i(\mathbf{x}; \theta_{\text{in}})$ is the activation of the i^{th} neuron. Since $a_i(\mathbf{x}; \theta_{\text{in}})$ is affine in \mathbf{x} , $\psi(a_i(\mathbf{x}; \theta_{\text{in}}))^2$ is a ‘rectified quadratic’ in \mathbf{x} and therefore convex. This completes the proof of theorem 2. In order to arrive at equation (3), we used that in both \mathcal{Q}_{FFG} and $\mathcal{Q}_{\text{MCDO}}$, the output weights of each neuron are independent. Correlations between the weights would introduce covariance terms which could be negative, leading to non-convex behaviour. Thus we see how *weight-space* factorisation assumptions can lead to *function-space* restrictions on the predictive uncertainty.

To complete the proof of theorem 1, we need to analyse $\mathbb{V}[\mathbb{E}[f(\mathbf{x})|\theta_{\text{in}}]]$ (equation (2)). Because of the factorisation assumptions on the weights in the first linear layer, this term can be expressed as a linear combination of the variances of each activation function. While these variances are not convex, we show that they satisfy restrictive conditions that allow us to provide bounds on arbitrary positive linear combinations of these functions. Full details of the proofs can be found in appendix A.

3.2. Empirical Tests of Approximate Inference

It is not immediately apparent that theorems 1 and 2 are problematic from the perspective of inference. For example, exact inference in Bayesian linear regression results in a convex variance function due to restrictive modelling assumptions. Here we provide strong evidence that the modelling assumptions of 1HL BNNs lead to exact posteriors that have in-between uncertainty. Theorems 1 and 2 thus imply that it is approximate inference with \mathcal{Q}_{FFG} or $\mathcal{Q}_{\text{MCDO}}$ that fails to reflect this intuitively desirable modelling assumption, violating **Criterion 1**.

While we cannot compute the exact posterior of a BNN, useful references can still be obtained for comparison. Specifically, we use two references: (1) Hamiltonian Monte Carlo (HMC) (Neal, 1995), a computationally expensive but accurate inference method that is often considered the gold standard; (2) exact Gaussian process (GP) inference with a kernel corresponding to the wide limit of the BNN (Neal, 1995; Lee et al., 2018; Matthews et al., 2018). Figure 3 compares the posterior predictive distributions obtained from MFVI, MCDO and the two references on a regression dataset consisting of two well separated clusters of covariates. We use 1HL BNNs with 50 hidden units and ReLU activations. The HMC and limiting GP posteriors are almost indistinguishable, suggesting that both methods are qualitatively similar to the exact posterior. For both these references $\mathbb{V}[f(\mathbf{x})]$ is markedly larger near the origin than near the data. In contrast, MFVI and MCDO are as confident in between the data as they are near the data. This provides strong evidence that the lack of in-between uncertainty is not a feature of the BNN model or prior, but is caused by approximate inference.

4. Deeper Networks

Theorems 1 and 2 pose an important question: is the structural limitation observed in the 1HL case fundamental to \mathcal{Q}_{FFG} and $\mathcal{Q}_{\text{MCDO}}$ even in deeper networks, or can depth

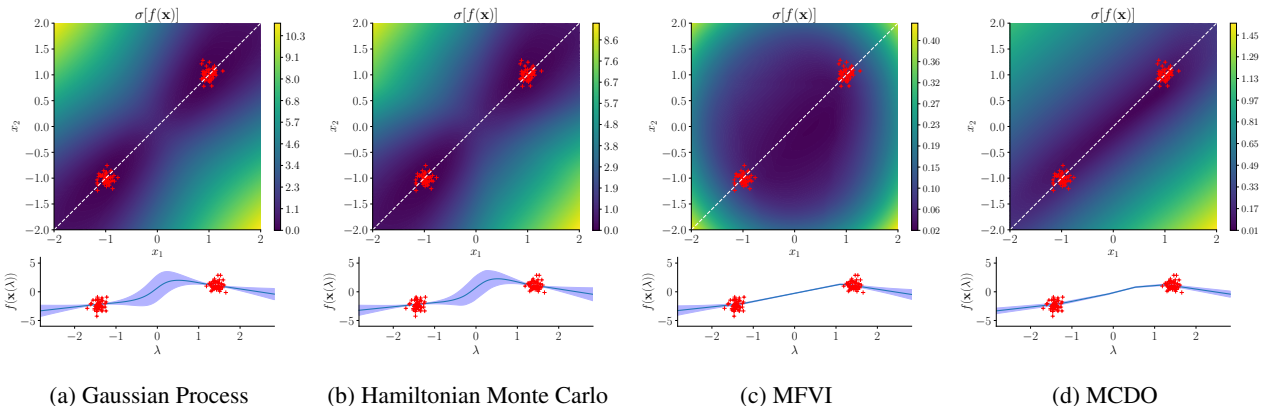


Figure 3. Regression on a 2D synthetic dataset (red crosses). The colour plots show the standard deviation, $\sigma[f(\mathbf{x})]$, of the output in different regions of input space. The plots beneath show the predictive mean with two-standard deviation bars along the dashed white line (parameterised by λ). Note MFVI and MCDO’s overconfidence in the region $\lambda \in [-1, 1]$. This behaviour is explained by theorems 1 and 2: given the uncertainty is near zero at the data clusters, there is *no* setting of the variational parameters that could have uncertainty significantly greater than zero in the line segment between them.

help these approximations satisfy **Criterion 1**? In theorem 3, we provide universality results for the mean and variance functions of BNNs with at least two hidden layers using \mathcal{Q}_{FFG} and $\mathcal{Q}_{\text{MCDO}}$. As the output mean and variance frequently determine the performance of BNNs in applications (e.g. in the acquisition functions for Bayesian optimisation or active learning), this provides theoretical evidence that approximate inference in deep BNNs satisfies **Criterion 1**.

Theorem 3 (Deeper networks). *Let g be any continuous function on a compact set $A \subset \mathbb{R}^D$, and h be any continuous, non-negative function on A . For any $\epsilon > 0$, for both mean-field Gaussian and MC dropout families there exists a 2-hidden layer ReLU BNN such that*

$$\sup_{\mathbf{x} \in A} |\mathbb{E}[f(\mathbf{x})] - g(\mathbf{x})| < \epsilon \text{ and } \sup_{\mathbf{x} \in A} |\mathbb{V}[f(\mathbf{x})] - h(\mathbf{x})| < \epsilon.$$

Remark 3. *If inputs are dropped out, the analogous statement to theorem 3 is false. In appendix D, we provide a simple counterexample that holds for arbitrarily deep networks showing that $\mathbb{V}[f]$ cannot be small at two points $\mathbf{x}_1, \mathbf{x}_2$ which have significantly different values of $\mathbb{E}[f(\mathbf{x}_1)]$ and $\mathbb{E}[f(\mathbf{x}_2)]$.*

Figure 4 shows the result of directly minimising the squared error between the network output mean and variance and a given target mean and variance function, using the same method and architecture as with the 1HL network in figure 2. In contrast to figure 2, the variances of both \mathcal{Q}_{FFG} and $\mathcal{Q}_{\text{MCDO}}$ are able to fit the target. While theorem 3 gives some cause for optimism for approximating family methods with deep BNNs, it only shows that the mean and variance of marginal distributions of the output are universal (e.g. it does not tell us about higher moments or covariances between

outputs), and it does not address **Criterion 2**.

4.1. Proof Sketch of Theorem 3

To prove theorem 3 for \mathcal{Q}_{FFG} , we provide a construction that relies on the universal approximation theorem for deterministic NNs (Leshno et al., 1993). Consider a 2HL NN whose second hidden layer has two neurons, with activations a_1, a_2 . Let w_1, w_2 denote the weights connecting a_1, a_2 to the output, and b denote the output bias, such that the output $f(\mathbf{x}) = w_1\psi(a_1) + w_2\psi(a_2) + b$, where we have suppressed the \mathbf{x} dependence in a_1, a_2 . In this construction, a_1 will be used to control the mean, and a_2 the variance, of the BNN output. By setting the variances in the first two linear layers to be sufficiently small, we can consider a_1 and a_2 as essentially deterministic functions of \mathbf{x} . By the universal approximation theorem, a_1 and a_2 can approximate any continuous functions. Choose $a_1 \approx g(\mathbf{x}) - \min_{\mathbf{x}' \in A} g(\mathbf{x}')$ and $a_2 \approx \sqrt{h(\mathbf{x})}$. Choose b to be essentially deterministic, with mean $\min_{\mathbf{x}' \in A} g(\mathbf{x}')$, w_1 to be essentially deterministic with mean 1 and w_2 to have mean 0 and variance 1. Then using linearity of expectation, the factorisation assumptions, and the non-negativity of a_1, a_2 :

$$\begin{aligned} \mathbb{E}[f(\mathbf{x})] &= \mathbb{E}[w_1\psi(a_1) + w_2\psi(a_2) + b] \\ &= \mathbb{E}[w_1] \mathbb{E}[\psi(a_1)] + \mathbb{E}[w_2] \mathbb{E}[\psi(a_2)] + \mathbb{E}[b] \\ &\approx g(\mathbf{x}) - \min_{\mathbf{x}' \in A} g(\mathbf{x}') + \min_{\mathbf{x}' \in A} g(\mathbf{x}') = g(\mathbf{x}), \end{aligned}$$

as desired. We can then calculate the variance of the network output using the law of total variance:

$$\begin{aligned} \mathbb{V}[f(\mathbf{x})] &= \mathbb{E}[\mathbb{V}[f(\mathbf{x})|a_1, a_2]] + \mathbb{V}[\mathbb{E}[f(\mathbf{x})|a_1, a_2]] \\ &\approx \mathbb{E}[\mathbb{V}[f(\mathbf{x})|a_1, a_2]] \\ &\approx \mathbb{E}[\psi(a_2)^2] + \mathbb{V}[b] \approx h(\mathbf{x}), \end{aligned}$$

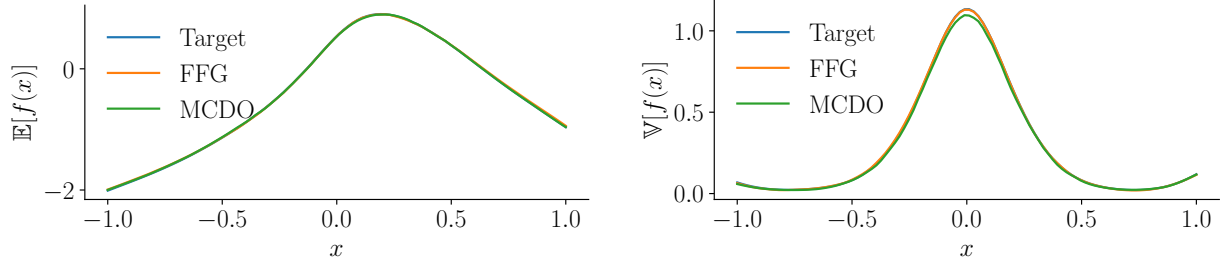


Figure 4. Results of minimising the squared error in function space between $\mathbb{E}[f(x)]$ and a target mean function (left), and between $\mathbb{V}[f(x)]$ and a target variance function (right), for a 2-hidden layer BNN with FFG and MCDO distributions. The target mean and variance functions were obtained from a wide-limit GP posterior. Both distributions are able to fit the target functions well, in contrast to the single-hidden layer case.

where we used that w_1, b are essentially deterministic and $\mathbb{V}[\mathbb{E}[f(\mathbf{x})|a_1, a_2]] \approx 0$ since a_1, a_2 are essentially deterministic. Also, we have that $\psi(a_2) \approx a_2$ since $a_2 \approx \sqrt{h(\mathbf{x})} \geq 0$. The approximations come from the standard universal function approximation theorem, and the variances of weights not being set exactly to 0 so that we remain in \mathcal{Q}_{FFG} . A rigorous proof, along with a proof for $\mathcal{Q}_{\text{MCDO}}$ with any dropout rate $p \in (0, 1)$, is given in appendix C. The proof for $\mathcal{Q}_{\text{MCDO}}$ uses a similar strategy, but is more involved as we are no longer able to set individual weights to be essentially deterministic.

4.2. Empirical Tests of Approximate Inference

We now consider empirically whether the distributions found *in practice* by VI with these families resemble the exact posterior in function-space, i.e. whether **Criterion 2** is satisfied. Figure 5 compares the uncertainty estimates obtained by MFVI and MCDO with those of the limiting GP and HMC for varying depths. We fix the BNN hidden layer width to 50. While neither the GP nor HMC performs exact inference in the finite BNN model, both act as useful references, and we expect the GP to retain qualitatively similar uncertainties to the exact BNN posterior.

A model with accurate inference should have similar uncertainty estimates to the limiting GP, i.e. the boxplot should be tightly centered around 1 (dashed line). On the 1HL and 2HL networks, the limiting GP and HMC agree closely, suggesting both resemble the exact posterior. In contrast, MFVI and MCDO are often an order of magnitude overconfident between the data clusters (the upper tail of the boxplot) and underconfident at the data clusters (the lower tail of the boxplot). Increased depth does not alleviate this behaviour. See appendix F for experimental details and additional figures demonstrating this for different priors.

In light of theorem 3 and figure 4 it is surprising that VI fails to capture important properties of the exact posterior with deep networks. This means that although **Criterion 1**

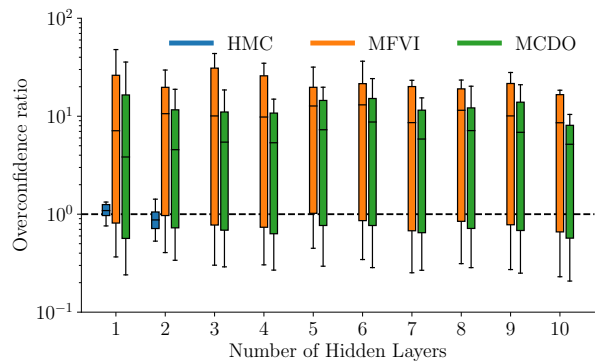


Figure 5. Boxplots of the overconfidence ratios of HMC, MFVI and MCDO relative to exact inference in an infinite width BNN (GP). We define the ‘overconfidence ratio’ at an input \mathbf{x} as $(\mathbb{V}_{\text{GP}}[f(\mathbf{x})]/\mathbb{V}_{q_\phi}[f(\mathbf{x})])^{1/2}$. We evaluate the overconfidence ratios on a discretisation of the segment of the white dotted line in figure 3 connecting the data clusters. HMC is only run for 1 and 2 hidden layers due to difficulty ensuring convergence in larger models.

may be satisfied for \mathcal{Q}_{FFG} and $\mathcal{Q}_{\text{MCDO}}$, **Criterion 2** is not met in practice. This may be due to the ELBO objective in weight-space being inappropriate for selecting good posteriors in function-space, or due to the optimiser finding poor local minima.

In appendix G we initialise the variational parameters at settings such that the approximate posterior in function-space has mean and variance functions that closely match a reference posterior that exhibits in-between uncertainty. This is done by directly minimising the squared loss between the BNN mean and variance functions and the reference mean and variance functions. We find that proceeding to optimise the ELBO from this initialisation still leads to a lack of in-between uncertainty. This suggests that the objective function is at least partially at fault for the mismatch between the approximate and exact posteriors.

| | 1 HL | 2 HL | 3 HL | 4 HL |
|-------------|--------------|--------------|--------------|--------------|
| GP Active | 0.040 ± 0.00 | 0.040 ± 0.00 | 0.044 ± 0.00 | 0.049 ± 0.00 |
| GP Random | 0.123 ± 0.01 | 0.137 ± 0.01 | 0.152 ± 0.01 | 0.167 ± 0.01 |
| MFVI Active | 0.732 ± 0.10 | 0.540 ± 0.03 | 0.449 ± 0.04 | 0.406 ± 0.03 |
| MFVI Random | 0.143 ± 0.01 | 0.238 ± 0.02 | 0.283 ± 0.02 | 0.327 ± 0.02 |
| MCDO Active | 0.729 ± 0.03 | 0.381 ± 0.02 | 0.481 ± 0.03 | 0.511 ± 0.02 |
| MCDO Random | 0.239 ± 0.02 | 0.346 ± 0.02 | 0.409 ± 0.02 | 0.443 ± 0.01 |

Table 1. Test RMSEs with ± 1 standard error after the 50th iteration of active learning, for different numbers of hidden layers (HL), averaged over 20 random seeds. Note that as the data is normalised, a method that predicts 0 will have an RMSE near 1.

5. Case Study: Active Learning with BNNs

We now consider the impact of the pathologies described in sections 3 and 4 on active learning (Settles, 2009) on a real-world dataset, where the task is to use uncertainty information to intelligently select which points to label. Active learning with approximate BNNs has been considered in previous works, often showing improvements over random selection of datapoints (Hernández-Lobato & Adams, 2015; Gal et al., 2017). However, when active learning fails, common metrics such as RMSE are insufficient to diagnose the causes. In particular, it is difficult to attribute the failure to the prior or to poor approximate inference. In this section, we provide a case study on active learning with BNNs on the Naval regression dataset (Coraddu et al., 2014), which is 16-dimensional and consists of 11,934 datapoints. The main questions we address are: i) Are theorems 1 and 2 indicative of pathological behaviour in the 1HL case? ii) Given theorem 3, will deeper approximate BNNs usefully reflect BNN modelling assumptions for active learning?

5.1. Experimental Set-up and Results

We compare MFVI, MCDO and the equivalent limiting GP.² We normalise the dataset to have zero mean and unit standard deviation. 5 datapoints are chosen randomly to form an initial active set, with the rest being the pool set. The models are trained on the active set, and we then choose the datapoint from the pool set that has the highest predictive variance, following Hernández-Lobato & Adams (2015). This point is added to the active set, and the process repeated 50 times. We then evaluate the RMSE of each model on a held-out test set, comparing to a baseline where points are chosen randomly. Full details are in appendix H.1.

The results are shown in table 1. We see that although active learning significantly reduces RMSE for the GP compared to random selection, it *increases* it for MFVI and MCDO. Although the performance of MFVI and MCDO improves somewhat with depth, active learning still fails to outperform the random baseline.

²HMC is too time-consuming to run on many iterations of active learning.

5.2. Discussion

We now consider if a pathology related to in-between uncertainty is responsible for the poor performance. In higher dimensional datasets such as Naval, it is not immediately apparent that theorems 1 and 2 are problematic, since convex hulls of sets of datapoints may have relatively low volume compared to in the 2D case. However, these theorems are likely to be symptomatic of *related* pathologies of 1HL BNN uncertainty estimates. To investigate this, in figure 6 we visualise the dataset using t-SNE (van der Maaten & Hinton, 2008). We see that the covariates of Naval are clustered, with points in the same cluster roughly the same distance from the origin. Since the dataset is mean-centred, points closer to the origin are in a sense ‘in between’ others.

In figure 6, we see that although the GP chooses points from almost every cluster during active learning, MFVI fails to select any points from many clusters — including all the clusters closest to the origin. It ignores points in the ‘inside’ and oversamples points on the ‘outside’, leading to a selection strategy worse than random. This behaviour is consistent with theorem 1. MCDO also fails to sample from many clusters; in appendix H.2 we show this is because it fails to reduce its uncertainty at clusters it has heavily sampled. Interestingly, it sometimes chooses from clusters near the origin, even though its variance function is provably convex. This could be because the minimum of the variance function for MCDO is not centred at the origin, or because the variance has the shape of an elongated valley. In contrast, the GP seems to select the ‘corners’ of each cluster, which is intuitively useful. The success of the GP provides strong evidence that the BNN model itself has desirable inductive biases for this task; it is approximate inference that has caused active learning to fail.

In deeper networks, we might hope that theorem 3 allows the BNN variance to be useful for active learning. However, although the problem is alleviated somewhat, MFVI still fails to choose points from some clusters close to the origin, and both methods fail to outperform the random baseline (see appendix H.2 and table 1). As this task only depends on marginal means and variances of the predictive distribution, **Criterion 1** is satisfied by theorem 3. Hence this demonstrates a failure of **Criterion 2** in the deep case.

6. Related Work

Concerns have been raised about the suitability of the Q_{FFG} family since the earliest work on BNNs. MacKay (1992, Figure 1) noted that a full-covariance Gaussian family was needed to obtain predictions with increased uncertainty away from data when using the Laplace approximation, although no detailed explanation was provided. The desire to go beyond Q_{FFG} has motivated a great deal of research

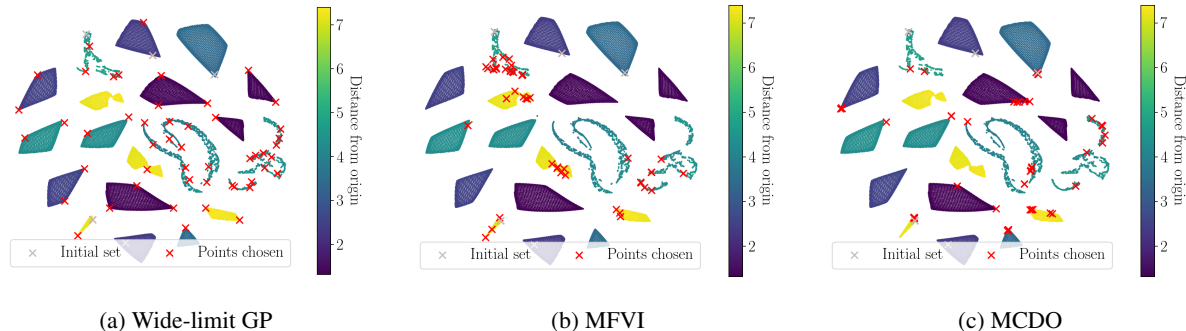


Figure 6. Points chosen during active learning in the 1HL case. Since t-SNE does not preserve relative positions, clusters near the origin may appear on the ‘outside’ of the t-SNE plot.

into more flexible approximating families (Barber & Bishop, 1998; Louizos & Welling, 2017; Ritter et al., 2018). However, to our knowledge, theorem 1 is the first theoretical result showing that \mathcal{Q}_{FFG} can have a pathologically restrictive effect on BNN predictive uncertainties.

Osband et al. (2018) note that the MCDO predictive distribution is invariant to duplicates of the data, and in the linear case predictive uncertainty does not decrease as dataset size increases (if the dropout rate and regulariser are fixed³). Theorem 2 allows us to show that in the non-linear 1HL case, predictive uncertainty in the MCDO posterior is fundamentally restricted even for datasets without repeated entries, regardless of the regulariser or dropout rate.

Farquhar et al. (2019) argued that MFVI becomes a less restrictive approximation as depth increases in BNNs. Their work primarily considers weight-space and provides an analysis of linear NNs, whereas we consider function-space and our theorems apply to the non-linear case. Although theorem 3 indicates that \mathcal{Q}_{FFG} with deep BNNs is indeed less restrictive, in sections 4 and 5 we find that *in practice* deep MFVI still fails to find solutions expressing adequate in-between uncertainty.

Alternative approaches to BNN inference consider directly targeting the predictive distribution in function-space (Sun et al., 2019; Shi et al., 2019; Ma et al., 2019). These methods treat the stochastic NN output as directly approximating the posterior stochastic process. Theorem 3 shows that to approximate both the predictive mean and variance well using \mathcal{Q}_{FFG} or $\mathcal{Q}_{\text{MCDO}}$, having at least 2 hidden layers is both necessary and sufficient, explaining a similar empirical observation in Sun et al. (2019), and providing a limited analogue of the universal approximation theorem (Leshno et al., 1993) in the stochastic setting.

³Note that for a fixed prior, the ‘KL condition’ (Gal, 2016, Section 3.2.3) requires the ℓ_2 regularisation constant to decrease with increasing dataset size.

7. Conclusions

We have presented both theoretical and empirical results characterising the expressiveness of the approximate posterior in function space obtained by MFVI and MCDO. For shallow BNNs we prove a fundamental limitation of mean-field Gaussian and MC dropout distributions on representing in-between uncertainty. While using deeper networks significantly improves the expressive power of these approximating families in terms of fitting arbitrary mean and variance functions, in practice VI does not take full advantage of this flexibility and again fails to capture in-between uncertainty.

To date, BNN approximate posteriors are poorly understood, especially when compared with the extensive work on understanding BNN priors (Neal, 1995; Lee et al., 2018; Matthews et al., 2018; Garriga-Alonso et al., 2019; Novak et al., 2019). Theorems 1 to 3 serve as an important first step in theoretically characterising the behaviour of approximate inference in these models. In order to understand the potential ramifications of Bayesian principles for deep learning, we need to understand the consequences of approximate inference as well as modelling assumptions. Characterising the successes and failure-modes of approximate inference requires not only simple summary metrics such as test log-likelihoods, but also diagnosing *which* qualities of the approximate posterior are responsible for performance. This is crucial if BNNs are to be used for safety-critical applications such as medical diagnosis (Esteva et al., 2017; Mobiny et al., 2019).

Theorem 3 raises important questions about the flexibility of approximate inference in deep networks: Can the theorem be extended to covariances or higher moments of the outputs? Why is **Criterion 2** not satisfied when performing VI in weight-space? We hope our results motivate future work to better understand the interaction between approximating families and objective functions, as well as new methods designed to realise the full potential of BNNs.

Acknowledgements

We thank Wessel Bruinsma for the proof of lemma 5, and José Miguel Hernández-Lobato, Ross Clarke and Sebastian W. Ober for helpful discussions. AYKF gratefully acknowledges funding from the Trinity Hall Research Studentship and the George and Lilian Schiff Foundation.

References

- Abramowitz, M. and Stegun, I. A. *Handbook of mathematical functions: with formulas, graphs, and mathematical tables*, volume 55. Courier Corporation, 1965.
- Barber, D. and Bishop, C. M. Ensemble learning in Bayesian neural networks. *NATO ASI Series F Computer and Systems Sciences*, 168:215–238, 1998.
- Beal, M. J. *Variational algorithms for approximate Bayesian inference*. PhD thesis, University College London, 2003.
- Bingham, E., Chen, J. P., Jankowiak, M., Obermeyer, F., Pradhan, N., Karaletsos, T., Singh, R., Szerlip, P., Horsfall, P., and Goodman, N. D. Pyro: Deep universal probabilistic programming. *Journal of Machine Learning Research (JMLR)*, 2018.
- Blei, D. M., Kucukelbir, A., and McAuliffe, J. D. Variational inference: A review for statisticians. *Journal of the American Statistical Association*, 112(518):859–877, 2017.
- Blundell, C., Cornebise, J., Kavukcuoglu, K., and Wierstra, D. Weight uncertainty in neural networks. In *International Conference on Machine Learning (ICML)*, 2015.
- Coraddu, A., Oneto, L., Ghio, A., Savio, S., Anguita, D., and Figari, M. Machine learning approaches for improving condition-based maintenance of naval propulsion plants. *Journal of Engineering for the Maritime Environment*, 2014.
- Deisenroth, M. and Rasmussen, C. E. PILCO: A model-based and data-efficient approach to policy search. In *International Conference on Machine Learning (ICML)*, pp. 465–472, 2011.
- Denker, J. S. and Lecun, Y. Transforming neural-net output levels to probability distributions. In *Advances in Neural Information Processing Systems (NIPS)*, 1991.
- Esteva, A., Kuprel, B., Novoa, R. A., Ko, J., Swetter, S. M., Blau, H. M., and Thrun, S. Dermatologist-level classification of skin cancer with deep neural networks. *Nature*, 542(7639):115, 2017.
- Farquhar, S., Smith, L., and Gal, Y. Try depth instead of weight correlations: Mean-field is a less restrictive assumption for variational inference in deep networks. In *Bayesian Deep Learning, NeurIPS Workshop*, 2019.
- Filos, A., Farquhar, S., Gomez, A. N., Rudner, T. G. J., Kenton, Z., Smith, L., Alizadeh, M., de Kroon, A., and Gal, Y. Benchmarking Bayesian deep learning with diabetic retinopathy diagnosis. <https://github.com/OATML/bdl-benchmarks>, 2019.
- Fort, S., Hu, H., and Lakshminarayanan, B. Deep ensembles: A loss landscape perspective. *arXiv preprint arXiv:1912.02757*, 2019.
- Frey, B. J. and Hinton, G. E. Variational learning in nonlinear Gaussian belief networks. *Neural Computation*, 11(1):193–213, 1999.
- Gal, Y. *Uncertainty in deep learning*. PhD thesis, University of Cambridge, 2016.
- Gal, Y. and Ghahramani, Z. Dropout as a Bayesian approximation: Representing model uncertainty in deep learning. In *International Conference on Machine Learning (ICML)*, 2016.
- Gal, Y., Islam, R., and Ghahramani, Z. Deep Bayesian active learning with image data. In *International Conference on Machine Learning (ICML)*, 2017.
- Garriga-Alonso, A., Rasmussen, C. E., and Aitchison, L. Deep convolutional networks as shallow Gaussian processes. In *International Conference on Learning Representations (ICLR)*, 2019.
- Hernández-Lobato, J. M. and Adams, R. Probabilistic back-propagation for scalable learning of Bayesian neural networks. In *International Conference on Machine Learning (ICML)*, 2015.
- Hernández-Lobato, J. M., Li, Y., Rowland, M., Bui, T., Hernández-Lobato, D., and Turner, R. Black-box alpha divergence minimization. In *International Conference on Machine Learning (ICML)*, 2016.
- Hinton, G. E. and Van Camp, D. Keeping the neural networks simple by minimizing the description length of the weights. In *Conference on Computational learning theory (COLT)*, 1993.
- Hoffman, M. D. and Gelman, A. The No-U-Turn sampler: adaptively setting path lengths in Hamiltonian Monte Carlo. *Journal of Machine Learning Research (JMLR)*, 15(1):1593–1623, 2014.
- Hron, J., Matthews, A., and Ghahramani, Z. Variational Bayesian dropout: Pitfalls and fixes. In *International Conference on Machine Learning (ICML)*, 2018.

- Jordan, M. I., Ghahramani, Z., Jaakkola, T. S., and Saul, L. K. An introduction to variational methods for graphical models. *Machine Learning*, 37(2):183–233, 1999.
- Khan, M. E., Nielsen, D., Tangkaratt, V., Lin, W., Gal, Y., and Srivastava, A. Fast and scalable Bayesian deep learning by weight-perturbation in Adam. *International Conference on Machine Learning (ICML)*, 2018.
- Kingma, D. P. and Welling, M. Auto-encoding variational Bayes. In *International Conference on Learning Representations (ICLR)*, 2014.
- Kingma, D. P., Salimans, T., and Welling, M. Variational dropout and the local reparameterization trick. In *Advances in Neural Information Processing Systems (NIPS)*, pp. 2575–2583, 2015.
- Lee, J., Sohl-dickstein, J., Pennington, J., Novak, R., Schoenholz, S., and Bahri, Y. Deep neural networks as Gaussian processes. In *International Conference on Learning Representations (ICLR)*, 2018.
- Leshno, M., Lin, V. Y., Pinkus, A., and Schocken, S. Multilayer feedforward networks with a nonpolynomial activation function can approximate any function. *Neural Networks*, 6(6):861–867, 1993.
- Li, Y. and Turner, R. E. Rényi divergence variational inference. In *Advances in Neural Information Processing Systems (NIPS)*, pp. 1073–1081, 2016.
- Li, Y., Hernández-Lobato, J. M., and Turner, R. E. Stochastic expectation propagation. In *Advances in Neural Information Processing Systems (NIPS)*, pp. 2323–2331, 2015.
- Louizos, C. and Welling, M. Multiplicative normalizing flows for variational Bayesian neural networks. In *International Conference on Machine Learning (ICML)*, 2017.
- Ma, C., Li, Y., and Hernández-Lobato, J. M. Variational implicit processes. In *International Conference on Machine Learning (ICML)*, 2019.
- MacKay, D. J. C. A practical Bayesian framework for backpropagation networks. *Neural Computation*, 4(3): 448–472, 1992.
- Matthews, A., Hron, J., Rowland, M., Turner, R. E., and Ghahramani, Z. Gaussian process behaviour in wide deep neural networks. In *International Conference on Learning Representations (ICLR)*, 2018.
- Matthews, A. G. d. G., van der Wilk, M., Nickson, T., Fujii, K., Boukouvalas, A., León-Villagrà, P., Ghahramani, Z., and Hensman, J. GPflow: A Gaussian process library using TensorFlow. *Journal of Machine Learning Research (JMLR)*, 18(40):1–6, 2017.
- Mobiny, A., Singh, A., and Van Nguyen, H. Risk-aware machine learning classifier for skin lesion diagnosis. *Journal of Clinical Medicine*, 8(8):1241, 2019.
- Neal, R. M. *Bayesian learning for neural networks*. PhD thesis, University of Toronto, 1995.
- Novak, R., Xiao, L., Bahri, Y., Lee, J., Yang, G., Abolafia, D. A., Pennington, J., and Sohl-dickstein, J. Bayesian deep convolutional networks with many channels are Gaussian processes. In *International Conference on Learning Representations (ICLR)*, 2019.
- Osawa, K., Swaroop, S., Khan, M. E. E., Jain, A., Eschenhagen, R., Turner, R. E., and Yokota, R. Practical deep learning with Bayesian principles. In *Advances in Neural Information Processing Systems (NeurIPS)*, pp. 4289–4301, 2019.
- Osband, I. Risk versus uncertainty in deep learning: Bayes, bootstrap and the dangers of dropout. In *Bayesian Deep Learning, NIPS workshop*, 2016.
- Osband, I., Aslanides, J., and Cassirer, A. Randomized prior functions for deep reinforcement learning. In *Advances in Neural Information Processing Systems (NeurIPS)*, pp. 8617–8629, 2018.
- Ovadia, Y., Fertig, E., Ren, J., Nado, Z., Sculley, D., Nowozin, S., Dillon, J. V., Lakshminarayanan, B., and Snoek, J. Can you trust your model’s uncertainty? Evaluating predictive uncertainty under dataset shift. In *Advances in Neural Information Processing Systems (NeurIPS)*, 2019.
- Ritter, H., Botev, A., and Barber, D. A scalable Laplace approximation for neural networks. In *International Conference on Learning Representations (ICLR)*, 2018.
- Schoenholz, S. S., Gilmer, J., Ganguli, S., and Sohl-Dickstein, J. Deep information propagation. In *International Conference on Learning Representations (ICLR)*, 2017.
- Settles, B. Active learning literature survey. Technical report, University of Wisconsin-Madison Department of Computer Sciences, 2009.
- Shi, J., Khan, M. E., and Zhu, J. Scalable training of inference networks for Gaussian-process models. In *International Conference on Machine Learning (ICML)*, 2019.
- Springenberg, J. T., Klein, A., Falkner, S., and Hutter, F. Bayesian optimization with robust Bayesian neural networks. In *Advances in Neural Information Processing Systems (NIPS)*, 2016.

- Srivastava, N., Hinton, G., Krizhevsky, A., Sutskever, I., and Salakhutdinov, R. Dropout: a simple way to prevent neural networks from overfitting. *Journal of Machine Learning Research (JMLR)*, 15(1):1929–1958, 2014.
- Sun, S., Zhang, G., Shi, J., and Grosse, R. Functional variational Bayesian neural networks. In *International Conference on Learning Representations (ICLR)*, 2019.
- Tomczak, M. B., Swaroop, S., and Turner, R. E. Neural network ensembles and variational inference revisited. In *1st Symposium on Advances in Approximate Bayesian Inference (AABI)*, 2018.
- van der Maaten, L. and Hinton, G. Visualizing data using t-SNE. *Journal of Machine Learning Research (JMLR)*, 9:2579–2605, 2008.

A. General Statements and Proofs of Theorems 1 and 2

In section 3 we stated simplified versions of bounds concerning the variance of single-hidden layer networks with certain approximating families. The two main results we prove in this section are the following generalisations of theorems 1 and 2 respectively:

Theorem 1. Consider a single-hidden layer ReLU neural network mapping from $\mathbb{R}^D \rightarrow \mathbb{R}^K$ with $I \in \mathbb{N}$ hidden units. The corresponding mapping is given by $f^{(k)}(\mathbf{x}) = \sum_{i=1}^I w_{k,i} \psi \left(\sum_{d=1}^D u_{i,d} x_d + v_i \right) + b_k$ for $1 \leq k \leq K$, where $\psi(a) = \max(0, a)$. Suppose we have a distribution over network parameters with density of the form:

$$q(\mathbf{W}, \mathbf{b}, \mathbf{U}, \mathbf{v}) = \prod_{i=1}^I q_i(\mathbf{w}_i | \mathbf{U}, \mathbf{v}) q(\mathbf{b} | \mathbf{U}, \mathbf{v}) \prod_{i=1}^I \prod_{d=1}^D \mathcal{N}(u_{i,d}; \mu_{u_{i,d}}, \sigma_{u_{i,d}}^2) \prod_{i=1}^I \mathcal{N}(v_i; \mu_{v_i}, \sigma_{v_i}^2), \quad (4)$$

where $\mathbf{w}_i = \{w_{k,i}\}_{k=1}^K$ are the weights out of neuron i and $\mathbf{b} = \{b_k\}_{k=1}^K$ are the output biases, and $q_i(\mathbf{w}_i | \mathbf{U}, \mathbf{v})$ and $q(\mathbf{b} | \mathbf{U}, \mathbf{v})$ are arbitrary probability densities with finite first two moments. Consider a line in \mathbb{R}^D parameterised by $\mathbf{x}(\lambda)_d = \gamma_d \lambda + c_d$ for $\lambda \in \mathbb{R}$ such that $\gamma_d c_d = 0$ for $1 \leq d \leq D$. Then for any $\lambda_1 \leq 0 \leq \lambda_2$, and any λ_* such that $|\lambda_*| \leq \min(|\lambda_1|, |\lambda_2|)$,

$$\mathbb{V}[f^{(k)}(\mathbf{x}(\lambda_*))] \leq \mathbb{V}[f^{(k)}(\mathbf{x}(\lambda_1))] + \mathbb{V}[f^{(k)}(\mathbf{x}(\lambda_2))] \quad \text{for } 1 \leq k \leq K. \quad (5)$$

We now briefly show how the statement of theorem 1 in the main text can be deduced from this more general version. The fully factorised Gaussian family \mathcal{Q}_{FFG} is of the form in equation (4). It remains to show that both conditions *i.* and *ii.* imply that $\gamma_d c_d = 0$. Consider any line intersecting the origin (i.e. satisfying condition *i.*). Such a line can be written in the form $\mathbf{x}(\lambda)_d = \gamma_d \lambda$ by choosing the origin to correspond to $\lambda = 0$. As $c_d = 0$ for all d , $\gamma_d c_d = 0$ for all d . In theorem 1 $\mathbf{p} = \mathbf{x}(\lambda_1)$ and $\mathbf{q} = \mathbf{x}(\lambda_2)$ are on opposite sides of the origin, hence the signs of λ_1 and λ_2 are opposite. Finally, the condition that $\mathbf{r} = \mathbf{x}(\lambda_*)$ is closer to the origin than both \mathbf{p} and \mathbf{q} is exactly that $|\lambda_*| \leq \min(|\lambda_1|, |\lambda_2|)$.

In order to verify condition *ii.*, note that any line orthogonal to a hyperplane $x_{d'} = 0$ can be parameterised as $\mathbf{x}(\lambda)_d = \gamma_d \lambda + c_d$, where $\gamma_d = 0$ for $d \neq d'$ and $c_{d'} = 0$. Hence $\gamma_d c_d = 0$ for all d . The condition that the line segment $\overrightarrow{\mathbf{p}\mathbf{q}}$ intersects the plane, with $\mathbf{p} = \mathbf{x}(\lambda_1)$ and $\mathbf{q} = \mathbf{x}(\lambda_2)$ is exactly that the signs of λ_1 and λ_2 are opposite, and that $|\lambda_*| \leq \min(|\lambda_1|, |\lambda_2|)$.

As a corollary of theorem 1, we can obtain bounds on higher-dimensional objects than lines, such as on hypercubes. For instance, consider the case where $\mathbf{x} \in \mathbb{R}^2$. Let $\mathbf{p}, \mathbf{q}, \mathbf{r}, \mathbf{s}$ be the four corners of a rectangle centered the origin. For any point \mathbf{a} in the rectangle, we can upper bound $\mathbb{V}[f(\mathbf{a})]$ by the sum of the variances at the top and bottom edges of the rectangle. These in turn can be upper bounded by the variances at the corners of the rectangle. Hence we have that for any point \mathbf{a} in the rectangle, $\mathbb{V}[f(\mathbf{a})] \leq \mathbb{V}[f(\mathbf{p})] + \mathbb{V}[f(\mathbf{q})] + \mathbb{V}[f(\mathbf{r})] + \mathbb{V}[f(\mathbf{s})]$. Similarly the variance at any point in a hypercube centered at the origin can be bounded by the sum of the variances on its vertices, and we can obtain tighter bounds on diagonals and faces of the hypercube, by repeatedly applying theorem 1.

Theorem 2 (MC dropout). Consider a single-hidden layer ReLU neural network mapping from $\mathbb{R}^D \rightarrow \mathbb{R}^K$ with $I \in \mathbb{N}$ hidden units. The corresponding mapping is given by $f^{(k)}(\mathbf{x}) = \sum_{i=1}^I w_{k,i} \psi \left(\sum_{d=1}^D u_{i,d} x_d + v_i \right) + b_k$ for $1 \leq k \leq K$, where $\psi(a) = \max(0, a)$. Assume \mathbf{U}, \mathbf{v} are set deterministically and

$$q(\mathbf{W}, \mathbf{b}) = q(\mathbf{b}) \prod_{i=1}^I q_i(\mathbf{w}_i),$$

where $\mathbf{w}_i = \{w_{k,i}\}_{k=1}^K$ are the weights out of neuron i , $\mathbf{b} = \{b_k\}_{k=1}^K$ are the output biases and $q(\mathbf{b})$ and $q_i(\mathbf{w}_i)$ are arbitrary probability densities with finite first two moments. Then, $\mathbb{V}[f^{(k)}(\mathbf{x})]$ is convex in \mathbf{x} for $1 \leq k \leq K$.

Proof. The theorem follows immediately from lemma 1 since \mathbf{U} and \mathbf{v} are deterministic. \square

Remark 4. Theorem 2 applies for any activation function ψ such that ψ^2 is convex. This is the only property of ψ used in lemma 1.

A.1. Preliminary Lemmas

In order to prove theorems 1 and 2 we first collect a series of preliminary lemmas.

Lemma 1. Assume a distribution for $\mathbf{W}, \mathbf{b}|\mathbf{U}, \mathbf{v}$ with density of the form

$$q(\mathbf{W}, \mathbf{b}|\mathbf{U}, \mathbf{v}) = q(\mathbf{b}|\mathbf{U}, \mathbf{v}) \prod_i q_i(\mathbf{w}_i|\mathbf{U}, \mathbf{v}).$$

Then, $\mathbb{V}[f^{(k)}(\mathbf{x})|\mathbf{U}, \mathbf{v}]$ is a convex function of \mathbf{x} .

The proof of lemma 1 is in appendix B.1.

Lemma 2. Consider the variance of a single neuron in the one dimensional case, with activation $a(x) \sim \mathcal{N}(\mu(x), \sigma^2(x))$, $\mu(x) = \mu_u x + \mu_v$, and $\sigma^2(x) = \sigma_u^2 x^2 + \sigma_v^2$. Let

$$\mathcal{T}_1 = \{f \geq 0 : \forall 0 \leq b < a, f(a) \geq f(-a) \text{ and } f(b) \leq f(a)\}$$

and

$$\mathcal{T}_2 = \{f \geq 0 : \forall a < b \leq 0, f(a) \geq f(-a) \text{ and } f(b) \leq f(a)\}.$$

If $\mu_u \geq 0$, then $\mathbb{V}[\psi(a(x))]\in \mathcal{T}_1$. If $\mu_u \leq 0$, then $\mathbb{V}[\psi(a(x))]\in \mathcal{T}_2$.

The proof of lemma 2 is in appendix B.2.

Corollary 1 (Corollary of lemma 2). Consider a line in \mathbb{R}^D parameterized by $[\mathbf{x}(\lambda)]_d = \gamma_d \lambda + c_d$ for $\lambda \in \mathbb{R}$ such that $\gamma_d c_d = 0$ for $1 \leq d \leq D$. Let $a(\mathbf{x}) := \sum_{d=1}^D u_d x_d + v$ with $\{u_d\}_{d=1}^D$ and v independent and Gaussian distributed. Then, $\mathbb{V}[\psi(a(\mathbf{x}(\lambda)))] \in \mathcal{T}_1 \cup \mathcal{T}_2$ (as a function of λ).

Proof. The activation $a(\mathbf{x}(\lambda))$ is a linear combination of Gaussian random variables, and is therefore Gaussian distributed. Moreover the mean is linear in λ . The variance of $a(\mathbf{x}(\lambda))$ is given by:

$$\begin{aligned} \mathbb{V}[a(\mathbf{x}(\lambda))] &= \sum_{d=1}^D \mathbb{V}[u_d(\gamma_d \lambda + c_d)]^2 + \mathbb{V}[v] \\ &= \sum_{d=1}^D \sigma_{u_d}^2 (\gamma_d \lambda + c_d)^2 + \sigma_v^2 \\ &= \lambda^2 \left(\sum_{d=1}^D \sigma_{u_d}^2 \gamma_d^2 \right) + 2\lambda \left(\sum_{d=1}^D \sigma_{u_d}^2 \gamma_d c_d \right) + \left(\sum_{d=1}^D \sigma_{u_d}^2 c_d^2 + \sigma_v^2 \right) \\ &= \lambda^2 \left(\sum_{d=1}^D \sigma_{u_d}^2 \gamma_d^2 \right) + \left(\sum_{d=1}^D \sigma_{u_d}^2 c_d^2 + \sigma_v^2 \right) \end{aligned}$$

Defining $\sigma_u^2 = \sum_{d=1}^D \sigma_{u_d}^2 \gamma_d^2$ and $\sigma_v^2 = \sum_{d=1}^D \sigma_{u_d}^2 c_d^2 + \sigma_v^2$, the corollary follows from lemma 2. \square

Lemma 3. Let \mathcal{C} be the set of convex functions from $\mathbb{R} \rightarrow [0, \infty)$. Fix any $a < 0 < b$ and c such that $|c| \leq \min(|a|, |b|)$. Then any function f that can be written as a linear combination of functions in $\mathcal{T}_1 \cup \mathcal{T}_2 \cup \mathcal{C}$ with non-negative weights satisfies, $f(c) \leq f(a) + f(b)$.

The proof of lemma 3 can be found in appendix B.3.

A.2. Proof of Theorem 1

Having collected the necessary preliminary lemmas we now prove theorem 1.

Proof of theorem 1. By the law of total variance,

$$\mathbb{V}[f^{(k)}(\mathbf{x})] = \mathbb{E}[\mathbb{V}[f^{(k)}(\mathbf{x})|\mathbf{U}, \mathbf{v}]] + \mathbb{V}[\mathbb{E}[f^{(k)}(\mathbf{x})|\mathbf{U}, \mathbf{v}]].$$

Using lemma 1, $\mathbb{V}[f^{(k)}(\mathbf{x})|\mathbf{U}, \mathbf{v}]$ is convex as a function of \mathbf{x} . As the expectation of a convex function is convex, the first term is a convex function of \mathbf{x} . For the second term we have

$$\mathbb{E}[f^{(k)}(\mathbf{x})|\mathbf{U}, \mathbf{v}] = \mathbb{E}\left[\sum_{i=1}^I w_{k,i}\psi(a_i) + b_k \middle| \mathbf{U}, \mathbf{v}\right] = \sum_{i=1}^I \mu_{w_{k,i}}\psi(a_i) + \mu_{b_k},$$

where $\mu_{w_{k,i}} := \mathbb{E}[w_{k,i}]$, $\mu_{b_k} := \mathbb{E}[b_k]$. In the second line we used linearity of expectation and that conditioned on (\mathbf{U}, \mathbf{v}) , the a_i are deterministic. Next,

$$\mathbb{V}[\mathbb{E}[f^{(k)}(\mathbf{x})|\mathbf{U}, \mathbf{v}]] = \mathbb{V}\left[\sum_{i=1}^I \mu_{w_{k,i}}\psi(a_i) + \mu_{b_k}\right] = \sum_{i=1}^I \mu_{w_{k,i}}^2 \mathbb{V}[\psi(a_i)], \quad (6)$$

since the a_i are independent of each other.

Consider a line in \mathbb{R}^D parameterised by $[\mathbf{x}(\lambda)]_d = \gamma_d\lambda + c_d$ for $\lambda \in \mathbb{R}$ such that $\gamma_d c_d = 0$ for $1 \leq d \leq D$.

By corollary 1, $\mathbb{V}[\psi(a_i(\mathbf{x}(\lambda)))] \in \mathcal{T}_1 \cup \mathcal{T}_2$ (as a function of λ). Since $\mathbb{V}[f^{(k)}(\mathbf{x})|\mathbf{U}, \mathbf{v}]$ is convex as a function of \mathbf{x} , it is also convex as a function of λ . We have written $\mathbb{V}[f^{(k)}(\mathbf{x}(\lambda))]$ in the form assumed in lemma 3, completing the proof. \square

B. Proof of Lemmas

In this section we prove the preliminary lemmas stated in appendix A.1.

B.1. Proof of Lemma 1

Proof. We assume a distribution for the network weights such that:

$$q(\mathbf{W}, \mathbf{b}|\mathbf{U}, \mathbf{v}) = q(\mathbf{b}|\mathbf{U}, \mathbf{v}) \prod_{i=1}^I q_i(\mathbf{w}_i|\mathbf{U}, \mathbf{v}).$$

By this factorisation assumption, the outgoing weights from each neuron are conditionally independent. This means the conditional variance of the output under this distribution can be written

$$\mathbb{V}[f^{(k)}(\mathbf{x})|\mathbf{U}, \mathbf{v}] = \sum_i \mathbb{V}[w_{k,i}|\mathbf{U}, \mathbf{v}]\psi(a_i)^2 + \mathbb{V}[b_k|\mathbf{U}, \mathbf{v}]. \quad (7)$$

with $a_i := a_i(\mathbf{x}) = \sum_{d=1}^D u_{i,d}x_d + v_i$.

Since $\mathbb{V}[f^{(k)}(\mathbf{x})|\mathbf{U}, \mathbf{v}]$ is a linear combination of the $\psi(a_i)^2$ with non-negative weights (plus a constant), to prove convexity it suffices to show that each $\psi(a_i)^2$ is convex as a function of \mathbf{x} . $\psi(a_i)^2$ is convex as a function of a_i , since it is 0 for $a_i \leq 0$ and a_i^2 for $a_i > 0$. To show that it is convex as a function of \mathbf{x} , we write

$$\begin{aligned} \psi(a_i(t\mathbf{x}_1 + (1-t)\mathbf{x}_2))^2 &= \psi\left(\sum_d u_{i,d}(t[\mathbf{x}_1]_d + (1-t)[\mathbf{x}_2]_d) + v_i\right)^2 \\ &= \psi\left(t\left(\sum_d u_{i,d}[\mathbf{x}_1]_d + v_i\right) + (1-t)\left(\sum_d u_{i,d}[\mathbf{x}_2]_d + v_i\right)\right)^2 \\ &\leq t\psi\left(\sum_d u_{i,d}[\mathbf{x}_1]_d + v_i\right)^2 + (1-t)\psi\left(\sum_d u_{i,d}[\mathbf{x}_2]_d + v_i\right)^2 \\ &= t\psi(a_i(\mathbf{x}_1))^2 + (1-t)\psi(a_i(\mathbf{x}_2))^2. \end{aligned}$$

The inequality uses convexity of $\psi(a)$ as a function of a . \square

B.2. Proof of Lemma 2

Throughout, we assume σ_u, σ_v and μ_v are fixed and suppress dependence on these parameters. Let $v_{\mu_u}(x) := \mathbb{V}[\psi(a(x))]$ where the variance is taken with respect to a distribution with parameter μ_u . Then, $v_{\mu_u}(x) = v_{-\mu_u}(-x)$ since $\mu(x)$ and $\sigma^2(x)$ are unchanged by the transformation $\mu_u, x \rightarrow -\mu_u, -x$.

Suppose $v_{\mu_u} \in \mathcal{T}_1$ for $\mu_u > 0$, then for $x \leq 0$,

$$v_{-\mu_u}(x) = v_{\mu_u}(-x) \geq v_{\mu_u}(x) = v_{-\mu_u}(-x),$$

and for $x < y \leq 0$,

$$v_{-\mu_u}(y) = v_{\mu_u}(-y) \leq v_{\mu_u}(-x) = v_{-\mu_u}(x).$$

In words, if $v_{\mu_u} \in \mathcal{T}_1$ then $v_{-\mu_u} \in \mathcal{T}_2$. It therefore suffices to consider the case when $\mu_u \geq 0$.

We first show that if $x \geq 0$, $v_{\mu_u}(x) \geq v_{\mu_u}(-x)$. Henceforth, we assume $\mu_u \geq 0$ is fixed and suppress it notationally. From [Frey & Hinton \(1999\)](#),

$$v(x) = \sigma(x)^2 \alpha(r(x)), \quad (8)$$

Here $r(x) = \mu(x)/\sigma(x)$. We define $h(r) = N(r) + r\Phi(r)$, where N is the standard Gaussian pdf, Φ is the standard Gaussian cdf. We define $\alpha(r) = \Phi(r) + rh(r) - h(r)^2$.

As $\sigma(x)^2 = \sigma(-x)^2$, it suffices to show $\alpha(r(x)) \geq \alpha(r(-x))$ for $x > 0$. To show this, we first show that $r(x) \geq r(-x)$ for $x > 0$, then show that $\alpha(r)$ is monotonically increasing.

$$r(x) = \mu(x)/\sigma(x) = \mu(-x)/\sigma(-x) + 2\mu_u x/\sigma(-x) \geq \mu(-x)/\sigma(-x) = r(-x).$$

The inequality uses that both μ_u and x are non-negative. It remains to show that $\alpha(r)$ is monotonically increasing. A straightforward calculation shows that,

$$\alpha'(r) = 2h(r)(1 - \Phi(r)).$$

As $1 - \Phi(r) > 0$, we must show $h(r) \geq 0$. We have $\lim_{r \rightarrow -\infty} h(r) = 0$ and $h'(r) = \Phi(r) > 0$, implying $h(r) > 0$. We conclude $\alpha'(r) > 0$ for all r , showing that $v_{\mu_u}(x) \geq v_{\mu_u}(-x)$ for $x \geq 0$.

To complete the proof, we must show that $v(x)$ is monotonically increasing for $x \geq 0$. As $\sigma(x)^2$ is increasing as a function of x and $\alpha(r)$ is increasing as a function of r , $v(x)$ is increasing as a function of x whenever $r(x)$ is increasing as a function of x . As $r'(x) = \frac{\sigma_v^2 \mu_u - \sigma_u^2 \mu_v x}{\sigma(x)^3}$, this completes the proof if $\sigma_v^2 \mu_u - \sigma_u^2 \mu_v x \geq 0$. In particular, we need only consider cases when $\mu_v > 0$. In this case, we write,

$$v(x) = \mu(x)^2 \beta(r(x)) \quad (9)$$

where $\beta(r) = \alpha(r)/r^2$. Also in this region, we have the inequality,

$$r'(x)\sigma(x) = \frac{\sigma_v^2 \mu_u - \sigma_u^2 \mu_v x}{\sigma_u^2 x^2 + \sigma_v^2} \leq \frac{\sigma_v^2 \mu_u}{\sigma_u^2 x^2 + \sigma_v^2} \leq \frac{\sigma_v^2 \mu_u}{\sigma_v^2} = \mu_u,$$

which leads to $r'(x) \leq \mu_u/\sigma(x)$.

Differentiating equation (9),

$$v'(x) = 2\mu_u \mu(x) \beta(r(x)) + \mu(x)^2 \left(\frac{\sigma_v^2 \mu_u - \sigma_u^2 \mu_v x}{\sigma(x)^3} \right) \beta'(r(x)) \geq 2\mu_u \mu(x) \left(\beta(r(x)) + \frac{1}{2} r(x) \beta'(r(x)) \right).$$

The inequality uses that $r(x) > 0$, so that by lemma 4, $\beta'(r(x)) < 0$. It suffices to show that $\beta(r) + \frac{1}{2} r \beta'(r) > 0$ for $r > 0$.

$$\beta(r) + \frac{1}{2} r \beta'(r) = \beta(r) + \frac{1}{2} r \frac{d}{dr} \left(\frac{\alpha(r)}{r^2} \right) = \frac{\alpha(r)}{r^2} + \frac{1}{2} r \frac{\alpha'(r)r^2 - 2r\alpha(r)}{r^4} = \frac{\alpha'(r)}{2r} \geq 0.$$

We conclude that $v'(x) \geq 0$ for $x \geq 0$, implying that $v(x)$ is monotonically increasing in this region. This completes the proof that $v_{\mu_u}(x) \in \mathcal{T}_1$ for $\mu_u > 0$.

Lemma 4. For β defined as in the proof of lemma 2 and for $r > 0$, $\beta'(r) < 0$

Proof. For $r \neq 0$, $\beta'(r) = \frac{-2\Phi(r) + 2N(r)^2 + 2N(r)\Phi(r)}{r^3}$. As $r > 0$,

$$\beta'(r) \leq 0 \Leftrightarrow I(r) := -\Phi(r) + N(r)^2 + N(r)r\Phi(r) \leq 0.$$

Rearranging (Abramowitz & Stegun, 1965, 7.1.13) yields:

$$1 - \frac{2}{r + \sqrt{r^2 + 8/\pi}}N(r) \leq \Phi(r) < 1 - \frac{2}{r + \sqrt{r^2 + 4}}N(r). \quad (10)$$

for $r \geq 0$.

$$\begin{aligned} I(r) &= -\Phi(r) + N(r)^2 + rN(r)\Phi(r) \\ &\leq -\Phi(r) + N(r)^2 + rN(r) \left(1 - \frac{2}{r + \sqrt{r^2 + 4}}N(r)\right) \\ &\leq -1 + \frac{2}{r + \sqrt{r^2 + 8/\pi}}N(r) + N(r)^2 + rN(r) \left(1 - \frac{2}{r + \sqrt{r^2 + 4}}N(r)\right) \\ &= -1 + \frac{2}{r + \sqrt{r^2 + 8/\pi}}N(r) + rN(r) + N(r)^2 \left(1 - \frac{2r}{r + \sqrt{r^2 + 4}}\right) \end{aligned} \quad (11)$$

We now make use of numerous crude bounds which hold for $r > 0$:

$$\text{i. } N(r) \leq 1/\sqrt{2\pi}, \quad \text{ii. } \frac{2}{r + \sqrt{r^2 + 8/\pi}} \leq \sqrt{\pi/2}, \quad \text{iii. } rN(r) \leq 1/\sqrt{2\pi e} \quad \text{iv. } \frac{2r}{r + \sqrt{r^2 + 4}} \geq 0.$$

Plugging these into equation (11),

$$I(r) \leq -1 + \frac{\sqrt{\pi/2}}{\sqrt{2\pi}} + \frac{1}{\sqrt{2\pi e}} + \frac{1}{2\pi} = -\frac{1}{2} + \frac{1}{\sqrt{2\pi e}} + \frac{1}{2\pi} \approx -0.098 < 0. \quad \square$$

B.3. Proof of Lemma 3

Proof. Recall that

$$\mathcal{T}_1 = \{f \geq 0 : \forall 0 \leq b < a, f(a) \geq f(-a) \text{ and } f(b) \leq f(a)\}$$

and

$$\mathcal{T}_2 = \{f \geq 0 : \forall a < b \leq 0, f(a) \geq f(-a) \text{ and } f(b) \leq f(a)\}.$$

First, note that $\mathcal{T}_1, \mathcal{T}_2$ and the set of non-negative convex functions, \mathcal{C} are all closed under addition and positive scalar multiplication. We can therefore write f as a sum of three functions, $f(x) = t_1(x) + t_2(x) + s(x)$ with $t_1 \in \mathcal{T}_1, t_2 \in \mathcal{T}_2$ and $s \in \mathcal{C}$. We prove the case when $a \leq c \leq 0 \leq -c \leq b$. The case $a \leq -c \leq 0 \leq c \leq b$ follows a symmetric argument.

$$\begin{aligned} f(c) &= t_1(c) + t_2(c) + s(c) \quad (\text{def.}) \\ &\leq t_1(c) + t_2(a) + s(c) \quad (\text{second condition for } \mathcal{T}_2) \\ &\leq t_1(-c) + t_2(a) + s(c) \quad (\text{first condition for } \mathcal{T}_1) \\ &\leq t_1(b) + t_2(a) + s(c) \quad (\text{second condition for } \mathcal{T}_1) \\ &\leq t_1(b) + t_2(a) + \max(s(a), s(b)) \quad (s \text{ convex}) \\ &\leq t_1(b) + t_2(a) + s(a) + s(b) \\ &\leq t_1(a) + t_1(b) + t_2(a) + t_2(b) + s(a) + s(b) \quad (\text{non-negativity}) \\ &= f(a) + f(b). \end{aligned} \quad \square$$

C. Proof of Theorem 3

We now restate and prove Theorem 3 from the main body:

Theorem 3. *Let $A \subset \mathbb{R}^D$ be compact, and let $C(A)$ be the space of continuous functions on A to \mathbb{R} . Similarly, let $C^+(A)$ be the space of continuous functions on A to $\mathbb{R}_{\geq 0}$. Then for any $g \in C(A)$ and $h \in C^+(A)$, and any $\epsilon > 0$, for both the mean-field Gaussian and MC dropout families, there exists a 2-hidden layer ReLU NN such that*

$$\sup_{\mathbf{x} \in A} |\mathbb{E}[f(\mathbf{x})] - g(\mathbf{x})| < \epsilon \quad \text{and} \quad \sup_{\mathbf{x} \in A} |\mathbb{V}[f(\mathbf{x})] - h(\mathbf{x})| < \epsilon,$$

where $f(\mathbf{x})$ is the (stochastic) output of the network.

Our proof will make use of the standard universal approximation theorem for deterministic NNs as given in Leshno et al. (1993):

Theorem 4 (Universal approximation for deterministic NNs). *Let $\psi(a) = \max(0, a)$. Then for every $g \in C(\mathbb{R}^D)$ and every compact set $A \subset \mathbb{R}^D$, for any $\epsilon > 0$ there exists a function $f \in S$ such that $\|g - f\|_\infty < \epsilon$. Here*

$$S = \left\{ \sum_{i=1}^I w_i \psi \left(\sum_{d=1}^D u_{i,d} x_d + v_i \right) : I \in \mathbb{N}, w_i, u_{i,d}, v_i \in \mathbb{R} \right\}.$$

We first prove a useful lemma.⁴

Lemma 5. *Let $\psi(a) = \max(0, a)$. Let a be a random variable with finite first two moments. Then $\mathbb{V}[\psi(a)] \leq \mathbb{V}[a]$.*

Proof. For all $x, y \in \mathbb{R}$, we have $|x - y|^2 \geq |\psi(x) - \psi(y)|^2$. Consider two i.i.d. copies of any random variable with finite first two moments, denoted a_1 and a_2 . Then

$$\mathbb{V}[a_1] = \mathbb{E}[a_1^2] - \mathbb{E}[a_1]^2 = \frac{1}{2} \mathbb{E}[a_1^2 + a_2^2 - 2a_1 a_2] = \frac{1}{2} \mathbb{E}[|a_1 - a_2|^2] \geq \frac{1}{2} \mathbb{E}[|\psi(a_1) - \psi(a_2)|^2] = \mathbb{V}[\psi(a_1)]. \quad \square$$

C.1. Proof of Theorem 3 for \mathcal{Q}_{FFG}

We prove theorem 3 for the fully-factorised Gaussian approximating family. We begin by proving results about 1HL networks within this family. These networks will be used to construct the desired 2HL network.

Notation Consider a 1HL ReLU NN with input $\mathbf{x} \in \mathbb{R}^D$ and output $\mathbf{f} \in \mathbb{R}^K$. Let the network have I hidden units and be parameterised by input weights $U \in \mathbb{R}^{I \times D}$, input biases $v \in \mathbb{R}^I$, output weights $W \in \mathbb{R}^{K \times I}$ and output biases $b \in \mathbb{R}^K$. Let $\theta = (U, v, W, b)$. Denote the k^{th} output of the network by $f_\theta^{(k)}(\mathbf{x})$. Consider a factorised Gaussian distribution over the parameters θ in the network. Let the means of the Gaussians be denoted $\boldsymbol{\mu} = (\mu_U, \mu_v, \mu_W, \mu_b)$, where e.g. μ_U is a matrix whose elements are the means of U . Each mean is always taken to be $\in \mathbb{R}$. Let the standard deviations be denoted $\boldsymbol{\sigma} = (\sigma_U, \sigma_v, \sigma_W, \sigma_b)$. Each standard deviation is always taken to be $\in \mathbb{R}_{>0}$.

The following lemma states that we can make the output of a 1HL BNN have low variance by setting the standard deviation of the weights to be small.

Lemma 6. *Let $A \subset \mathbb{R}^D$ be a compact set and $f_\theta^{(k)}(\mathbf{x})$ be the k^{th} output of a 1HL ReLU NN with a mean-field Gaussian distribution mapping from $A \rightarrow \mathbb{R}$. Fix any $\boldsymbol{\mu}$ and any $\epsilon > 0$. Let all the standard deviations in $\boldsymbol{\sigma}$ be equal to a shared constant $\sigma > 0$. Then there exists $\sigma' > 0$ such that for all $\sigma < \sigma'$ and for all $\mathbf{x} \in A$, $\mathbb{V}[\psi(f_\theta^{(k)}(\mathbf{x}))] < \epsilon$ for all $1 \leq k \leq K$.*

⁴The proof of this lemma is due to Wessel Bruinsma.

Proof. Define $a_i = \sum_{d=1}^D u_{i,d}x_d + v_i$, so that $f_\theta^{(k)}(\mathbf{x}) = \sum_{i=1}^I w_{k,i}\psi(a_i) + b_k$. Then

$$\begin{aligned} \mathbb{V}[f_\theta^{(k)}(\mathbf{x})] &= \mathbb{V}\left[\sum_{i=1}^I w_{k,i}\psi(a_i)\right] + \sigma^2 \\ &= \sum_{i=1}^I \sum_{j=1}^I \text{Cov}(w_{k,i}\psi(a_i), w_{k,j}\psi(a_j)) + \sigma^2 \\ &\leq \sum_{i=1}^I \sum_{j=1}^I |\text{Cov}(w_{k,i}\psi(a_i), w_{k,j}\psi(a_j))| + \sigma^2 \\ &\leq \sum_{i=1}^I \sum_{j=1}^I \sqrt{\mathbb{V}[w_{k,i}\psi(a_i)]\mathbb{V}[w_{k,j}\psi(a_j)]} + \sigma^2, \end{aligned}$$

where the final line follows from the Cauchy–Schwarz inequality. We now analyse each of the constituent terms. Since $w_{k,i}$ and $\psi(a_i)$ are independent,

$$\mathbb{V}[w_{k,i}\psi(a_i)] = \mu_{w_{k,i}}^2 \mathbb{V}[\psi(a_i)] + \mathbb{E}[\psi(a_i)]^2 \sigma^2 + \sigma^2 \mathbb{V}[\psi(a_i)].$$

As A is compact, it is bounded, so there exists an M such that $|x_d| \leq M$ for all $1 \leq d \leq D$. Using lemma 5, and the mean-field assumptions,

$$\mathbb{V}[\psi(a_i)] \leq \mathbb{V}[a_i] = \sigma^2 \left(\sum_{d=1}^D x_d^2 + 1 \right) \leq \sigma^2 (DM^2 + 1).$$

Since a_i is a linear combination of Gaussian random variables, we have that $a_i \sim \mathcal{N}(\mu_{a_i}, \sigma_{a_i}^2)$, where $\mu_{a_i} = \sum_{d=1}^D \mu_{u_{i,d}}x_d + \mu_{v_i}$ and $\sigma_{a_i}^2 = \sigma^2 \left(\sum_{d=1}^D x_d^2 + 1 \right)$. Therefore, we have that (Frey & Hinton, 1999)

$$\mathbb{E}[\psi(a_i)]^2 = \left(\mu_{a_i} \Phi\left(\frac{\mu_{a_i}}{\sigma_{a_i}}\right) + \sigma_{a_i} N\left(\frac{\mu_{a_i}}{\sigma_{a_i}}\right) \right)^2 \leq \left(|\mu_{a_i}| \Phi\left(\frac{\mu_{a_i}}{\sigma_{a_i}}\right) + \sigma_{a_i} N\left(\frac{\mu_{a_i}}{\sigma_{a_i}}\right) \right)^2 \leq \left(|\mu_{a_i}| + \frac{\sigma_{a_i}}{\sqrt{2\pi}} \right)^2.$$

We can then upper bound $\mathbb{V}[w_{k,i}\psi(a_i)]$ as follows:

$$\begin{aligned} \mathbb{V}[w_{k,i}\psi(a_i)] &\leq \mu_{w_{k,i}}^2 \sigma^2 (DM^2 + 1) + \left(|\mu_{a_i}| + \frac{\sigma_{a_i}}{\sqrt{2\pi}} \right)^2 \sigma^2 + \sigma^4 (DM^2 + 1) \\ &\leq \mu_{w_{k,i}}^2 \sigma^2 (DM^2 + 1) + \left(M \sum_{d=1}^D |\mu_{u_{i,d}}| + |\mu_{v_i}| + \frac{\sqrt{\sigma^2 (M^2 D + 1)}}{\sqrt{2\pi}} \right)^2 \sigma^2 + \sigma^4 (DM^2 + 1) := v_{k,i}(\sigma). \end{aligned}$$

The second inequality follows since A is compact and we have $|\mu_{a_i}| \leq M \sum_{d=1}^D |\mu_{u_{i,d}}| + |\mu_{v_i}|$. Note that the upper bound $v_{k,i}(\sigma)$ is continuous and monotonically increasing in σ , and $v_{k,i}(0) = 0$. We can then upper bound the variance of the output:

$$\mathbb{V}[f_\theta^{(k)}(\mathbf{x})] \leq \sum_{i=1}^I \sum_{j=1}^I \sqrt{v_{k,i}(\sigma)v_{k,j}(\sigma)} + \sigma^2.$$

We then choose σ' such that for all $1 \leq k \leq K$ and for all $1 \leq i \leq I$, $v_{k,i}(\sigma') < \frac{\epsilon}{2I^2}$, and such that $\sigma'^2 < \frac{\epsilon}{2}$. Then

$$\mathbb{V}[f_\theta^{(k)}(\mathbf{x})] \leq I^2 \frac{\epsilon}{2I^2} + \sigma'^2 < \epsilon$$

for $1 \leq k \leq K$. Finally, applying lemma 5, we have $\mathbb{V}[\psi(f_\theta^{(k)}(\mathbf{x}))] < \epsilon$ for $1 \leq k \leq K$. \square

The following lemma states that by setting the standard deviation of the weights to be sufficiently small, we can with high probability make the sampled BNN output close to the BNN output evaluated at the mean parameters.

Lemma 7. *Let $A \subset \mathbb{R}^D$ be any compact set. Fix any $\boldsymbol{\mu}$ and any $\epsilon, \delta > 0$. Let all the standard deviations in $\boldsymbol{\sigma}$ be equal to a shared constant $\sigma > 0$. Then there exists $\sigma' > 0$ such that for all $\sigma < \sigma'$, and for any $\mathbf{x} \in A$,*

$$\Pr \left(|\psi(f_{\boldsymbol{\mu}}^{(k)}(\mathbf{x})) - \psi(f_{\boldsymbol{\theta}}^{(k)}(\mathbf{x}))| > \epsilon \right) < \delta$$

for all $1 \leq k \leq K$.

Proof. Let $\theta \in \mathbb{R}^P$. We first note that $\psi(f_{\boldsymbol{\theta}}^{(k)}(\mathbf{x}))$ is continuous as a function from $A \times \mathbb{R}^P \rightarrow \mathbb{R}$, under the metric topology induced by the Euclidean metric on $A \times \mathbb{R}^P$. Next, define a ball in parameter space

$$B_\gamma = \{\theta : \|\theta - \boldsymbol{\mu}\|_2 < \gamma\}.$$

Consider the closed ball of unit radius around $\boldsymbol{\mu}$, \bar{B}_1 . Note that \bar{B}_1 is compact, and therefore $A \times \bar{B}_1$ is compact as a product of compact spaces.

Since a continuous map from a compact metric space to another metric space is uniformly continuous, given $\epsilon > 0$, there exists a $0 < \tau < 1$ such that for all pairs $(\mathbf{x}_1, \theta_1), (\mathbf{x}_2, \theta_2) \in A \times \bar{B}_1$ such that $d((\mathbf{x}_1, \theta_1), (\mathbf{x}_2, \theta_2)) < \tau$, $|\psi(f_{\theta_1}^{(k)}(\mathbf{x}_1)) - \psi(f_{\theta_2}^{(k)}(\mathbf{x}_2))| < \epsilon$. Here $d(\cdot, \cdot)$ is the Euclidean metric on $A \times \mathbb{R}^P$. Since this is true for all $1 \leq k \leq K$, we can find a $0 < \tau < 1$ such that $|\psi(f_{\theta_1}^{(k)}(\mathbf{x}_1)) - \psi(f_{\theta_2}^{(k)}(\mathbf{x}_2))| < \epsilon$ holds for all k simultaneously, by taking the minimum of the τ over k .

Now choose $\sigma' > 0$ such that for all $\sigma < \sigma'$, $\Pr(\theta \in B_\tau) > 1 - \delta$. This event implies $d((\mathbf{x}, \theta), (\mathbf{x}, \boldsymbol{\mu})) = \|\theta - \boldsymbol{\mu}\|_2 < \tau$. Furthermore, $\theta \in \bar{B}_1$, since $\tau < 1$. Hence $|\psi(f_{\boldsymbol{\mu}}^{(k)}(\mathbf{x})) - \psi(f_{\boldsymbol{\theta}}^{(k)}(\mathbf{x}))| < \epsilon$ holds for all $1 \leq k \leq K$. □

The following lemma shows that for 1HL networks, we can make $\mathbb{E}[\psi(f_{\boldsymbol{\theta}}^{(k)})]$ (the mean BNN output) close to $\psi(f_{\boldsymbol{\mu}}^{(k)})$ (the BNN output evaluated at the mean parameter settings) by choosing the standard deviation of the weights to be sufficiently small.

Lemma 8. *Let $A \subset \mathbb{R}^D$ be any compact set. Then, for any $\epsilon > 0$ and any $\boldsymbol{\mu}$, there exists a $\sigma_1 > 0$ such that for any shared standard deviation $\sigma < \sigma_1$,*

$$\|\mathbb{E}[\psi(f_{\boldsymbol{\theta}}^{(k)})] - \psi(f_{\boldsymbol{\mu}}^{(k)})\|_\infty < \epsilon$$

for all $1 \leq k \leq K$.

Proof. For all $\mathbf{x} \in A$ and any θ^* , by the triangle inequality

$$\left| \mathbb{E}[\psi(f_{\boldsymbol{\theta}}^{(k)}(\mathbf{x}))] - \psi(f_{\boldsymbol{\mu}}^{(k)}(\mathbf{x})) \right| \leq \left| \mathbb{E}[\psi(f_{\boldsymbol{\theta}}^{(k)}(\mathbf{x}))] - \psi(f_{\boldsymbol{\theta}^*}^{(k)}(\mathbf{x})) \right| + \left| \psi(f_{\boldsymbol{\mu}}^{(k)}(\mathbf{x})) - \psi(f_{\boldsymbol{\theta}^*}^{(k)}(\mathbf{x})) \right|.$$

Applying lemma 7 with $\epsilon' = \epsilon/2$ and $\delta = 1/4$, we can find a σ' such that for all $\sigma < \sigma'$, $|\psi(f_{\boldsymbol{\mu}}^{(k)}(\mathbf{x})) - \psi(f_{\boldsymbol{\theta}^*}^{(k)}(\mathbf{x}))| \leq \epsilon/2$ with probability at least $3/4$. By lemma 6, we can find a σ'' such that for all $\sigma < \sigma''$, $\mathbb{V}[\psi(f_{\boldsymbol{\theta}}^{(k)}(\mathbf{x}))] < \frac{\epsilon^2}{16K}$. Choose $0 < \sigma < \min(\sigma', \sigma'')$. We can apply Chebyshev's inequality to each random variable $\psi(f_{\boldsymbol{\theta}}^{(k)}(\mathbf{x}))$,

$$\Pr[|\psi(f_{\boldsymbol{\theta}}^{(k)}(\mathbf{x})) - \mathbb{E}[\psi(f_{\boldsymbol{\theta}}^{(k)}(\mathbf{x}))]| > \epsilon/2] < \frac{1}{4K}.$$

Applying the union bound, the probability that $|\psi(f_{\boldsymbol{\theta}}^{(k)}(\mathbf{x})) - \mathbb{E}[\psi(f_{\boldsymbol{\theta}}^{(k)}(\mathbf{x}))]| \leq \epsilon/2$ for all k simultaneously is at least $3/4$.

Therefore, for any \mathbf{x} we can find a θ^* such that $|\psi(f_{\boldsymbol{\theta}^*}^{(k)}(\mathbf{x})) - \mathbb{E}[\psi(f_{\boldsymbol{\theta}}^{(k)}(\mathbf{x}))]| \leq \epsilon/2$ and $|\psi(f_{\boldsymbol{\mu}}^{(k)}(\mathbf{x})) - \psi(f_{\boldsymbol{\theta}^*}^{(k)}(\mathbf{x}))| \leq \epsilon/2$ simultaneously because both events occur with probability at least $1/2$ and therefore have a non-empty intersection. Therefore for all \mathbf{x} and all k

$$\left| \mathbb{E}[\psi(f_{\boldsymbol{\theta}}^{(k)}(\mathbf{x}))] - \psi(f_{\boldsymbol{\mu}}^{(k)}(\mathbf{x})) \right| \leq \epsilon. \quad \square$$

We can now complete the proof of theorem 3 for \mathcal{Q}_{FFG} .

Proof of theorem 3. Consider the case of a 2-hidden layer ReLU Bayesian neural network with 2 units in the second hidden layer. Denote the inputs to these units as $f_\theta^{(1)}(\mathbf{x})$ and $f_\theta^{(2)}(\mathbf{x})$ respectively, where θ are the parameters in the bottom two weight matrices and biases of the network. The output of the network can then be written as,

$$f(\mathbf{x}) = s_1\psi(f_\theta^{(1)}(\mathbf{x})) + s_2\psi(f_\theta^{(2)}(\mathbf{x})) + t \quad (12)$$

where the s_i are the weights in the final layer and t is the bias. Taking expectations on both sides,

$$\mathbb{E}[f(\mathbf{x})] = \mathbb{E}\left[s_1\psi(f_\theta^{(1)}(\mathbf{x}))\right] + \mathbb{E}\left[s_2\psi(f_\theta^{(2)}(\mathbf{x}))\right] + \mathbb{E}[t]$$

Choose $\mu_{s_1} = 1, \mu_{s_2} = 0$, and note that s_1 is independent of θ by the mean field assumption. Then

$$\mathbb{E}[f(\mathbf{x})] = \mathbb{E}\left[\psi(f_\theta^{(1)}(\mathbf{x}))\right] + \mathbb{E}[t].$$

Define $\mu_t = -\min_{\mathbf{x}' \in A} g(\mathbf{x}')$ (as A is compact and g is continuous, this minimum is well-defined). Define $\tilde{g}(\mathbf{x}) \geq 0$ to be $g(\mathbf{x}) - \min_{\mathbf{x}' \in A} g(\mathbf{x}')$. By the universal approximation theorem (theorem 4) we can find a setting of the mean parameters, $\boldsymbol{\mu}$ in the first two layers (i.e. excluding the parameters of the distributions on s_1, s_2 and t) such that

$$\|f_\mu^{(1)} - \tilde{g}\|_\infty < \epsilon/2 \quad \text{and} \quad \|f_\mu^{(2)} - \sqrt{h}\|_\infty < \epsilon/2.$$

This can be done by splitting the neurons in the first hidden layer into two sets, where the first and second set are responsible for $f^{(1)}, f^{(2)}$ respectively, and the weights from each set to the output of the other set are zero. Since $\tilde{g}(\mathbf{x}) > 0$, applying the ReLU can only make $f^{(1)}$ closer to \tilde{g} . Hence $\|\psi(f_\mu^{(1)}) - \tilde{g}\|_\infty < \epsilon/2$.

By lemma 8, we can find a $\sigma_1 > 0$ for this $\boldsymbol{\mu}$ such that when the standard deviations in the first two layers are set to any shared constant $\sigma < \sigma_1$,

$$\left\| \mathbb{E}\left[\psi(f_\theta^{(1)})\right] - \psi(f_\mu^{(1)}) \right\|_\infty < \epsilon/2.$$

By the triangle inequality, $\left\| \mathbb{E}\left[\psi(f_\theta^{(1)})\right] - \tilde{g} \right\|_\infty < \epsilon$. Combining with appendix C.1, it follows that the expectation can approximate any continuous function g .

We now consider the variance of equation (12).

$$\begin{aligned} \mathbb{V}[f(\mathbf{x})] &= \mathbb{V}[s_1\psi(f_\theta^{(1)}(\mathbf{x})) + s_2\psi(f_\theta^{(2)}(\mathbf{x}))] + \mathbb{V}[t] \\ &= \mathbb{V}[s_1\psi(f_\theta^{(1)}(\mathbf{x}))] + \mathbb{V}[s_2\psi(f_\theta^{(2)}(\mathbf{x}))] + 2\text{Cov}(s_1\psi(f_\theta^{(1)}(\mathbf{x})), s_2\psi(f_\theta^{(2)}(\mathbf{x}))) + \sigma_t^2. \end{aligned}$$

Choose $\sigma_t^2 = \epsilon$. We now consider $\mathbb{V}[s_1\psi(f_\theta^{(1)}(\mathbf{x}))]$. As s_1 is independent of θ ,

$$\mathbb{V}[s_1\psi(f_\theta^{(1)}(\mathbf{x}))] = \mu_{s_1}^2 \mathbb{V}[\psi(f_\theta^{(1)}(\mathbf{x}))] + \sigma_{s_1}^2 \mathbb{E}[\psi(f_\theta^{(1)}(\mathbf{x}))]^2 + \mathbb{V}[\psi(f_\theta^{(1)}(\mathbf{x}))]\sigma_{s_1}^2.$$

Recall $\mu_{s_1} = 1$ and choose $\sigma_{s_1}^2 = \min\left(1, \epsilon / \left(\max_{\mathbf{x} \in A} \mathbb{E}[\psi(f_\theta^{(1)}(\mathbf{x}))]^2\right)\right)$, then

$$\mathbb{V}[s_1\psi(f_\theta^{(1)}(\mathbf{x}))] \leq 2\mathbb{V}[\psi(f_\theta^{(1)}(\mathbf{x}))] + \epsilon.$$

By lemma 6, we can find a σ_2 such that for any $\sigma < \sigma_2$, $\mathbb{V}[\psi(f_\theta^{(1)}(\mathbf{x}))] \leq \epsilon$. For any such σ , $\mathbb{V}[s_1\psi(f_\theta^{(1)}(\mathbf{x}))] \leq 3\epsilon$.

We now choose $\sigma_{s_2}^2 = 1$ and consider

$$\mathbb{V}[s_2\psi(f_\theta^{(2)}(\mathbf{x}))] = \mu_{s_2}^2 \mathbb{V}[\psi(f_\theta^{(2)}(\mathbf{x}))] + \sigma_{s_2}^2 \mathbb{E}[\psi(f_\theta^{(2)}(\mathbf{x}))]^2 + \sigma_{s_2}^2 \mathbb{V}[\psi(f_\theta^{(2)}(\mathbf{x}))] = \mathbb{E}[\psi(f_\theta^{(2)}(\mathbf{x}))]^2 + \mathbb{V}[\psi(f_\theta^{(2)}(\mathbf{x}))].$$

By lemma 6, we can find a σ_3 such that for any $\sigma < \sigma_3$, $\mathbb{V}[\psi(f_\theta^{(2)}(\mathbf{x}))] < \epsilon$.

By the universal function approximator theorem (theorem 4) we can find a setting of the mean parameters, μ in the first two layers such that $\|f_{\mu}^{(2)} - \sqrt{h}\|_{\infty} < \epsilon/2$. Since $\sqrt{h(\mathbf{x})} > 0$, the ReLU can only make $f^{(2)}$ closer to \sqrt{h} , $\|\psi(f_{\mu}^{(2)}) - \sqrt{h}\|_{\infty} < \epsilon/2$.

By lemma 8, we can find a setting of σ for this μ such that

$$\left\| \mathbb{E} \left[\psi(f_{\theta}^{(2)}) \right] - \psi(f_{\mu}^{(2)}) \right\|_{\infty} < \epsilon/2.$$

By the triangle inequality,

$$\left\| \mathbb{E} \left[\psi(f_{\theta}^{(2)}) \right] - \sqrt{h} \right\|_{\infty} < \epsilon.$$

This implies,

$$\begin{aligned} \left\| \mathbb{E} \left[\psi(f_{\theta}^{(2)}) \right]^2 - h \right\|_{\infty} &= \left\| \left(\mathbb{E} \left[\psi(f_{\theta}^{(2)}) \right] - \sqrt{h} \right) \left(\mathbb{E} \left[\psi(f_{\theta}^{(2)}) \right] + \sqrt{h} \right) \right\|_{\infty} \\ &\leq \epsilon \left\| \mathbb{E} \left[\psi(f_{\theta}^{(2)}) \right] + \sqrt{h} \right\|_{\infty} \\ &\leq \epsilon(2\|\sqrt{h}\|_{\infty} + \epsilon) \end{aligned}$$

We therefore have,

$$\begin{aligned} \|\mathbb{V}[f] - h\|_{\infty} &\leq E(\epsilon) + 2\text{Cov}(s_1\psi(f_{\theta}^{(1)}(\mathbf{x})), s_2\psi(f_{\theta}^{(2)}(\mathbf{x}))) \\ &\leq E(\epsilon) + 2\sqrt{\mathbb{V}[s_1\psi(f_{\theta}^{(1)}(\mathbf{x}))]\mathbb{V}[s_2\psi(f_{\theta}^{(2)}(\mathbf{x}))]} \\ &\leq E(\epsilon) + C\sqrt{\epsilon} \end{aligned}$$

where the first inequality is Cauchy-Schwarz, and $E(\epsilon)$ is a function that tends to zero with ϵ and C is a constant. The theorem follows by choosing $\sigma < \min\{\sigma_1, \sigma_2, \sigma_3\}$. \square

The construction in our proof used a 2HL BNN with only two neurons in the second hidden layer. The construction still works for wider hidden layers, by setting the unused neurons to have zero mean and sufficiently small variance.

An analogous statement to theorem 3 for networks with more than two hidden layers can be proved inductively: applying theorem 3 for 2HL BNNs we can choose the variance to be uniformly small, thus satisfying the condition stated in lemma 6. The proof of lemma 7 applies equally for the output of 2HL BNNs. The rest of the proof then follows as stated.

C.2. Proof of theorem 3 for MCDO

In order to prove the universality result for deep dropout, we first prove two lemmas about 1HL dropout networks. The following lemma states that the mean of a 1HL dropout network is a universal function approximator, while its variance can simultaneously be made arbitrarily small.

Lemma 9. *Consider any $\epsilon > 0$ and any continuous function, m mapping from a compact subset, A of \mathbb{R}^D to \mathbb{R} . Then there exists a (random) ReLU neural network of the form*

$$f(x) = \sum_{i=1}^I w_i \gamma_i \psi \left(\sum_{d=1}^D u_{i,d} x_d + v_i \right) + b$$

with $\gamma_i \stackrel{\text{i.i.d.}}{\sim} \text{Bern}(1-p)$ such that $\|\mathbb{E}[f] - m\|_{\infty} < \epsilon$ and $\|\mathbb{V}[f]\|_{\infty} \leq \epsilon$.

Proof. By the universal approximation theorem [Leshno et al. \(1993\)](#), there exists a J and 1HL network of the form,

$$g(x) = \sum_{j=1}^J \tilde{w}_j \psi \left(\sum_{d=1}^D \tilde{u}_{j,d} x_d + v_j \right) + b,$$

such that $\|g - m\|_\infty \leq \epsilon$. Define the dropout network,

$$f^{(1)}(x) = \sum_{j=1}^J \frac{\tilde{w}_j}{1-p} \psi \left(\sum_{d=1}^D \tilde{u}_{j,d} x_d + v_j \right) + b.$$

Then $\mathbb{E}[f^{(1)}] = g$, so that $\|\mathbb{E}[f^{(1)}] - m\|_\infty \leq \epsilon$. Let $S = \|\mathbb{V}[f^{(1)}]\|_\infty < \infty$.

Define $f = \frac{1}{L} \sum_{\ell=1}^L f^{(1,\ell)}$ where each $f^{(1,\ell)}$ is an independent realisation of $f^{(1)}$. Then $\mathbb{E}[f] = g$ and $\mathbb{V}[f] = \frac{\mathbb{V}[f^{(1)}]}{\sqrt{L}} \leq \frac{S}{\sqrt{L}}$. f can be realised by a dropout network by combining L copies of $f^{(1)}$ together with identical weights within each copy and 0 weights connecting the various copies. Choosing $L = (S/\epsilon)^2$ completes the proof. \square

The following lemma states that the mean of the MCDO network can approximate any continuous *positive* function, after application of the ReLU non-linearity.

Lemma 10. *Given a positive mean function m with $0 < \delta \leq \|m\|_\infty \leq \Delta$ and a stochastic process f such that $\|\mathbb{E}[f] - m\|_\infty \leq \epsilon \leq \delta$ and $\|\mathbb{V}[f]\|_\infty \leq \epsilon$,*

$$\|\mathbb{E}[\psi(f)] - m\|_\infty \leq \epsilon + \frac{\sqrt{\epsilon^2 + \epsilon(\Delta + \epsilon)^2}}{\delta - \epsilon} = \mathcal{O}(\Delta\sqrt{\epsilon}/(\delta - \epsilon))$$

and $\|\mathbb{V}[\psi(f)]\|_\infty \leq \epsilon$. In the big- O notation, we assume Δ is bounded below by a constant and ϵ, δ are bounded above by a constant.

Proof. The bound $\|\mathbb{V}[\psi(f)]\|_\infty \leq \epsilon$ follows from lemma 5. We consider the expectation of $\psi(f(\mathbf{x}))$ for some arbitrary fixed \mathbf{x} ,

$$\begin{aligned} |\mathbb{E}[\psi(f(\mathbf{x}))] - m(\mathbf{x})| &= |\mathbb{E}[f(\mathbf{x})] - m(\mathbf{x}) - \mathbb{E}[\min(0, f(\mathbf{x}))]| \\ &\leq |\mathbb{E}[f(\mathbf{x})] - m(\mathbf{x})| + |\mathbb{E}[\min(0, f(\mathbf{x}))]| \\ &\leq \epsilon + |\mathbb{E}[\min(0, f(\mathbf{x}))]|. \end{aligned}$$

We therefore bound $|\mathbb{E}[\min(0, f(\mathbf{x}))]|$.

$$|\mathbb{E}[\min(0, f(\mathbf{x}))]| = |\mathbb{E}[f(\mathbf{x})\mathbf{1}\{\mathbf{x} : f(\mathbf{x}) < 0\}]| \leq \sqrt{\mathbb{E}[f(\mathbf{x})^2] \Pr(f(\mathbf{x}) < 0)}.$$

The inequality uses Cauchy-Schwarz, that the square of an indicator function is itself and reinterprets the expectation of an indicator function as a probability. We bound the two terms on the RHS separately.

$$\mathbb{E}[f(\mathbf{x})^2] = \mathbb{V}[f(\mathbf{x})] + \mathbb{E}[f(\mathbf{x})]^2 \leq \epsilon + \mathbb{E}[f(\mathbf{x})]^2 \leq \epsilon + (m(\mathbf{x}) + \epsilon)^2 \leq \epsilon + (\Delta + \epsilon)^2$$

We use Chebyshev's inequality to bound the probability $f(x) < 0$,

$$\Pr(f(\mathbf{x}) < 0) \leq \Pr(|f(\mathbf{x}) - \mathbb{E}[f(\mathbf{x})]| > m(\mathbf{x}) - \epsilon) \leq \frac{\mathbb{V}[f(\mathbf{x})]}{(m(\mathbf{x}) - \epsilon)^2} \leq \frac{\epsilon}{(m(\mathbf{x}) - \epsilon)^2} \leq \frac{\epsilon}{(\delta - \epsilon)^2}. \quad \square$$

Having collected the necessary lemmas, we provide a construction that proves theorem 3.

Proof of theorem 3. Consider a 2HL dropout NN. Let the pre-activations in the first hidden layer be collectively denoted \mathbf{a}_1 , and the random dropout masks by ϵ_1 . Let the second hidden layer have $I + 2$ hidden units. Let \odot denote the elementwise product of two vectors of the same length. Define the pre-activations of two of the second hidden layer units by $a_v = \mathbf{w}_v^T(\epsilon_1 \odot \psi(\mathbf{a}_1))$, i.e. both these hidden units have identical weight vectors \mathbf{w}_v and dropout masks, and are hence the same random variable. Similarly, let the remaining I second hidden layer pre-activations be defined by $a_m = \mathbf{w}_m^T(\epsilon_1 \odot \psi(\mathbf{a}_1))$, again all being the same random variable. Furthermore, let $(\mathbf{w}_v)_i = 0$ whenever $(\mathbf{w}_m)_i \neq 0$ and

vice versa, so that the first hidden layer neurons that influence a_v and those that influence a_m form disjoint sets. Then the output of the 2HL network is:

$$f = \epsilon_a w_{2,a} \psi(a_v) + \epsilon_b w_{2,b} \psi(a_v) + \sum_{i=1}^I \epsilon_i w_{2,i} \psi(a_m) + b_2,$$

where $\epsilon_a, \epsilon_b, \{\epsilon_i\}_{i=1}^I$ are the final layer dropout masks and $\{w_{2,i}\}_{i=1}^I, b_2$ are the final layer weights and bias.

We now make the choices $w_{2,a} = 1, w_{2,b} = -1, w_{2,i} = \alpha$, where $\alpha I = 1/(1-p)$. Then $\mathbb{E}[f] = \mathbb{E}[\psi(a_m)] + b_2$. Let $b_2 = \min_{x \in A} g - \delta$, where $\delta > 0$ and the min exists due to compactness of A . Define $g' = g - b_2$. Since a_m is just the output of a single-hidden layer dropout network, for any $\gamma' > 0$ we can use lemma 9 to choose $\|\mathbb{E}[a_m] - g'\|_\infty < \gamma'$ and $\|\mathbb{V}[a_m]\|_\infty < \gamma'$. Since g' is bounded below by δ and bounded above by some $\Delta \in \mathbb{R}$ (by continuity of g and compactness of A), we can then apply lemma 10 to obtain $\|\mathbb{E}[a_m] - g'\|_\infty = \mathcal{O}(\Delta \sqrt{\epsilon'} / (\delta - \epsilon'))$ and $\|\mathbb{V}[\psi(a_m)]\|_\infty < \gamma'$. We can use this to bound the error in the mean of the 2HL network output:

$$\|\mathbb{E}[f] - g\|_\infty = \|\mathbb{E}[\psi(a_m)] + b_2 - g\|_\infty = \|\mathbb{E}[\psi(a_m)] - g'\|_\infty = \mathcal{O}(\Delta \sqrt{\gamma'} / (\delta - \gamma')).$$

We can choose γ' to depend on δ, Δ such that $\|\mathbb{E}[f] - g\|_\infty < \gamma$, proving the first part of the theorem. Next, calculating the variance,

$$\mathbb{V}[f] = \mathbb{V} \left[(\epsilon_a - \epsilon_b) \psi(a_v) + \alpha \psi(a_m) \sum_{i=1}^I \epsilon_i \right] = \mathbb{V}[(\epsilon_a - \epsilon_b) \psi(a_v)] + \alpha^2 \mathbb{V} \left[\psi(a_m) \sum_{i=1}^I \epsilon_i \right] \quad (13)$$

Next we show that by taking I sufficiently large, we can make the second term arbitrarily small. We have,

$$\begin{aligned} \mathbb{V} \left[\psi(a_m) \sum_{i=1}^I \epsilon_i \right] &= \mathbb{V}[\psi(a_m)] \mathbb{V} \left[\sum_{i=1}^I \epsilon_i \right] + \mathbb{V}[\psi(a_m)] \mathbb{E} \left[\sum_{i=1}^I \epsilon_i \right]^2 + \mathbb{V} \left[\sum_{i=1}^I \epsilon_i \right] \mathbb{E}[\psi(a_m)]^2 \\ &= \mathbb{V}[\psi(a_m)] I p (1-p) + \mathbb{V}[\psi(a_m)] I^2 (1-p)^2 + I p (1-p) \mathbb{E}[\psi(a_m)]^2 \\ &\leq \gamma' I p (1-p) + \gamma' I^2 (1-p)^2 + I p (1-p) \mathbb{E}[\psi(a_m)]^2 \end{aligned}$$

The first two of these three terms can be made arbitrarily small by choosing γ' sufficiently small. The third term, upon multiplying by α^2 , becomes

$$\alpha^2 I p (1-p) \mathbb{E}[\psi(a_m)]^2 = \frac{p}{I(1-p)} \mathbb{E}[\psi(a_m)]^2,$$

which can also be made arbitrarily small by choosing $I \in \mathbb{N}$ sufficiently large. We now show that the first term in equation (13) can well approximate our target variance function h .

$$\mathbb{V}[(\epsilon_a - \epsilon_b) \psi(a_v)] = \mathbb{V}[\epsilon_a - \epsilon_b] \mathbb{V}[\psi(a_v)] + \mathbb{V}[\epsilon_a - \epsilon_b] \mathbb{E}[\psi(a_v)]^2 + \mathbb{V}[\psi(a_v)] \mathbb{E}[\epsilon_a - \epsilon_b]^2 \quad (14)$$

$$= 2p(1-p) \mathbb{V}[\psi(a_v)] + 2p(1-p) \mathbb{E}[\psi(a_v)]^2 \quad (15)$$

Define

$$h' = \sqrt{\frac{h}{2p(1-p)}} + \delta',$$

for some $\delta' > 0$. Again applying lemma 9 (which we can do independently of the choice of a_m since neurons influencing a_v and a_m are disjoint), for any $\gamma'' > 0$ we can choose $\|\mathbb{E}[a_v] - h'\|_\infty < \gamma''$ and $\|\mathbb{V}[a_v]\|_\infty < \gamma''$. The first term in equation (15) can be made arbitrarily small by choosing γ'' small enough. We can again apply lemma 10 so that $\|\mathbb{E}[\psi(a_v)] - h'\|_\infty = \mathcal{O}(\Delta' \sqrt{\gamma''} / (\delta' - \gamma''))$. We then bound the difference between the second term in equation (15) and our target variance function:

$$\left\| 2p(1-p) \mathbb{E}[\psi(a_v)]^2 - h \right\|_\infty \leq \left\| \sqrt{2p(1-p)} \mathbb{E}[\psi(a_v)] + \sqrt{h} \right\|_\infty \left\| \sqrt{2p(1-p)} \mathbb{E}[\psi(a_v)] - \sqrt{h} \right\|_\infty \quad (16)$$

$$\leq \left(\left\| 2\sqrt{h} \right\|_\infty + \left\| \sqrt{2p(1-p)} \mathbb{E}[\psi(a_v)] - \sqrt{h} \right\|_\infty \right) \left\| \sqrt{2p(1-p)} \mathbb{E}[\psi(a_v)] - \sqrt{h} \right\|_\infty \quad (17)$$

where equation (16) follows from sub-multiplicativity of the infinity norm. Expanding the second term in equation (17),

$$\left\| \sqrt{2p(1-p)} \mathbb{E}[\psi(a_v)] - \sqrt{h} \right\|_\infty = \sqrt{2p(1-p)} \|\mathbb{E}[\psi(a_v)] - h' + \delta'\|_\infty = \mathcal{O}(\delta' + \Delta' \sqrt{\gamma''}/(\delta' - \gamma''))$$

By first choosing δ' sufficiently small, and then choosing γ'' depending on δ' , we can make this error term arbitrarily small. Since all the other contributions to $\mathbb{V}[f]$ were made arbitrarily small, this allows us to set $\|\mathbb{V}[f] - h\| < \gamma$, for any $\gamma > 0$, completing the proof. \square

In order to provide an analogous construction for MCDO BNNs with more than 2 hidden layers, we note that the above proof only requires a BNN output with a universal mean function and an arbitrarily small variance function in lemma 9. Instead of a 1HL network, we can apply theorem 3 to construct a 2 or more hidden layer network to provide these mean and variance functions. The rest of the proof then follows as in the 2HL case.

D. Dropout With Inputs Dropped Out

The behaviour of MC dropout with inputs dropped out is somewhat different, both theoretically and empirically, from the case when inputs are not dropped out as discussed in the main body.

D.1. Single-Hidden Layer Networks

In the single-hidden layer case, the variance is no longer convex as a function of \mathbf{x} . On the other hand, this approximating family still struggles to represent in-between uncertainty:

Theorem 5 (MC dropout, dropped out inputs). *Consider a single-hidden layer ReLU neural network mapping from $\mathbb{R}^D \rightarrow \mathbb{R}^K$ with $I \in \mathbb{N}$ hidden units. The corresponding mapping is given by $f^{(k)}(\mathbf{x}) = \sum_{i=1}^I w_{k,i} \psi\left(\sum_{d=1}^D u_{i,d} x_d + v_i\right) + b_k$ for $1 \leq k \leq K$, where $\psi(a) = \max(0, a)$. Assume \mathbf{v} is set deterministically and*

$$q(\mathbf{W}, \mathbf{b}, \mathbf{U}) = q(\mathbf{U})q(\mathbf{b}|\mathbf{U}) \prod_i q_i(\mathbf{w}_i|\mathbf{U}),$$

where $\mathbf{w}_i = \{w_{k,i}\}_{k=1}^K$ are the weights out of neuron i , $\mathbf{b} = \{b_k\}_{k=1}^K$ are the output biases and $q(\mathbf{U})$, $q(\mathbf{b}|\mathbf{U})$ and $q_i(\mathbf{w}_i|\mathbf{U})$ are arbitrary probability densities with finite first two moments. Then, for any finite set of points $\mathcal{S} \subset \mathbb{R}^D$ such that $\mathbf{0}$ is in the convex hull of \mathcal{S} ,

$$\mathbb{V}[f^{(k)}(\mathbf{0})] \leq \max_{\mathbf{s} \in \mathcal{S}} \left\{ \mathbb{V}[f^{(k)}(\mathbf{s})] \right\} \quad \text{for } 1 \leq k \leq K. \quad (18)$$

In order to prove theorem 5 we use the following simple lemma,

Lemma 11. *Let $f : \mathbb{R}^D \rightarrow \mathbb{R}$ be a convex function and consider a finite set of points $\mathcal{S} \subset \mathbb{R}^D$. Then for any point \mathbf{r} in the convex hull of \mathcal{S} , $f(\mathbf{r}) \leq \max_{\mathbf{s} \in \mathcal{S}} \{f(\mathbf{s})\}$.*

Proof of lemma 11. Let $\{\mathbf{s}_n\}_{n=1}^N = \mathcal{S}_N \subset \mathbb{R}^D$. We proceed by induction. The lemma is true for $N = 2$ by the definition of convexity. Assume it is true for N . Let $\text{Conv}(\mathcal{S}_{N+1})$ denote the convex hull of \mathcal{S}_{N+1} . Consider a point $\mathbf{r}_{N+1} \in \text{Conv}(\mathcal{S}_{N+1})$. Then

$$f(\mathbf{r}_{N+1}) = f\left(\sum_{n=1}^{N+1} \alpha_n \mathbf{s}_n\right) \quad (19)$$

with $\sum_{n=1}^{N+1} \alpha_n = 1$ and $\alpha_n \geq 0$ for $1 \leq n \leq N+1$. We can write

$$f(\mathbf{r}_{N+1}) = f\left(\left(\sum_{n=1}^N \alpha_n\right) \mathbf{t}_N + \alpha_{N+1} \mathbf{s}_{N+1}\right) \leq \max\{f(\mathbf{t}_N), f(\mathbf{s}_{N+1})\} \quad (20)$$

where $\mathbf{t}_N := \sum_{n=1}^N \alpha_n \mathbf{s}_n / \sum_{n=1}^N \alpha_n$, and we have used the convexity of f . By the induction assumption, $f(\mathbf{t}_N) \leq \max_{\mathbf{s} \in \mathcal{S}_N} \{f(\mathbf{s})\}$, since $\mathbf{t}_N \in \text{Conv}(\mathcal{S}_N)$. Combining this with equation (20) completes the proof. \square

Proof of theorem 5. By the law of total variance,

$$\mathbb{V}[f^{(k)}(\mathbf{x})] = \mathbb{E}[\mathbb{V}[f^{(k)}(\mathbf{x})|\mathbf{U}]] + \mathbb{V}[\mathbb{E}[f^{(k)}(\mathbf{x})|\mathbf{U}]].$$

Using lemma 1, $\mathbb{V}[f^{(k)}(\mathbf{x})|\mathbf{U}]$ is convex as a function of \mathbf{x} . As the expectation of a convex function is convex, the first term is a convex function of \mathbf{x} . This implies

$$\mathbb{E}[\mathbb{V}[f^{(k)}(\mathbf{0})|\mathbf{U}]] \leq \max_{\mathbf{s} \in \mathcal{S}} \left\{ \mathbb{E}[\mathbb{V}[f^{(k)}(\mathbf{s})|\mathbf{U}]] \right\},$$

by lemma 11. $\mathbb{V}[\mathbb{E}[f^{(k)}(\mathbf{x})|\mathbf{U}]]$ is non-negative everywhere. As the output of the first layer is independent of the matrix \mathbf{U} at $\mathbf{x} = \mathbf{0}$, $\mathbb{E}[f^{(k)}(\mathbf{0})|\mathbf{U}]$ is deterministic. So $\mathbb{V}[\mathbb{E}[f^{(k)}(\mathbf{0})|\mathbf{U}]] = 0$, completing the proof. \square

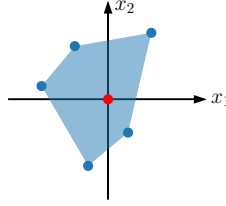


Figure 7. Schematic illustration of the bound in theorem 2, showing the input domain of a single-hidden layer MC dropout BNN, for the case $\mathbf{x} \in \mathbb{R}^2$. The convex hull (in blue) of the blue points contains the origin. Hence the variance at the origin cannot exceed the variance at any of the blue points.

D.2. Deep Networks

In the case when the network has several hidden layers, dropout with inputs dropped defines a posterior with somewhat strange properties, as observed in Gal (2016, Section 4.2.1). In particular, in D dimensions, a typical sample function from the approximate posterior will be constant as a function of roughly pD of the input dimensions. However, which dimensions it is constant along depends on the particular sample. This behaviour is unlikely to be shared by the exact posterior. We are able to exploit this type of behaviour to show that if inputs are dropped out, there are simple combinations of mean and variance functions that cannot be simultaneously approximated by the corresponding approximating family.

Proposition 1. Consider f the (stochastic) output of an MC dropout network of arbitrary depth with inputs dropped out. For any $x, x' \in \mathbb{R}$ such that $\mathbb{V}[f(x)], \mathbb{V}[f(x')] < \epsilon^2$, $|\mathbb{E}[f(x)] - \mathbb{E}[f(x')]| \leq 2\epsilon\sqrt{2/p}$.

Proof. With probability p , the input is dropped out, so $\Pr(f(x) = f(x')) \geq p$. We apply Chebyshev's inequality giving the bounds,

$$\Pr(|f(x) - \mathbb{E}[f(x)]| \leq r\epsilon) \geq 1 - 1/r^2 \quad \text{and} \quad \Pr(|f(x') - \mathbb{E}[f(x')]| \leq r\epsilon) \geq 1 - 1/r^2.$$

for any $r > 0$. Choose $r = \sqrt{2/p} + \delta$ for any $\delta > 0$, then there exists a realisation of the dropout network such that $|f(x) - \mathbb{E}[f(x)]| \leq r\epsilon$, $|f(x') - \mathbb{E}[f(x')]| \leq r\epsilon$ and $f(x) = f(x')$ simultaneously. Consequently,

$$\begin{aligned} |\mathbb{E}[f(x)] - \mathbb{E}[f(x')]| &= |\mathbb{E}[f(x)] - f(x) + f(x) - \mathbb{E}[f(x')]| \\ &= |\mathbb{E}[f(x)] - f(x) + f(x') - \mathbb{E}[f(x')]| \\ &\leq |\mathbb{E}[f(x)] - f(x)| + |f(x') - \mathbb{E}[f(x')]| \\ &\leq 2r\epsilon = 2\epsilon\sqrt{2/p} + 2\epsilon\delta. \end{aligned}$$

Taking the limit as $\delta \rightarrow 0$ completes the proof. \square

In other words we can bound the difference in the mean output at two points in terms of the uncertainty at those points and the dropout probability.

In $D > 1$ dimensions, we can get similarly tight bounds on lines parallel to a coordinate axis: for \mathbf{x}, \mathbf{x}' on such a line $\Pr(f(\mathbf{x}) = f(\mathbf{x}')) \geq p$ still holds. If the dimension on which \mathbf{x} and \mathbf{x}' differ is dropped out $f(\mathbf{x}) = f(\mathbf{x}')$.

Alternatively in D dimensions for arbitrary $\mathbf{x}, \mathbf{x}' \in \mathbb{R}^D$, $\Pr(f(\mathbf{x}) = f(\mathbf{x}')) \geq p^D$. This comes from noting that with probability p^D the output of the network is a constant function. However, we note this bound becomes exponentially weak as the input dimension increases.

E. Details for the Experiments Minimising Squared Loss

We generated a dataset that consisted of two separated clusters in one dimension. We then fit a Gaussian process to the dataset and computed the predictive mean and variance on a one-dimensional grid of $N = 40$ points, call these point X . Let $\mu(X) \in \mathbb{R}^N$ denote the mean of the GP regression at these points $\sigma^2(X) \in \mathbb{R}^N$ denote its variance. We define a loss function as

$$\mathcal{L}(\phi) = \|\mathbb{E}_{q_\phi}[f(X)] - \mu(X)\|_2^2 + \|\mathbb{V}_{q_\phi}[f(X)] - \sigma^2(X)\|_2^2.$$

The expectation and variance are Monte Carlo estimated using 128 samples. We use full batch optimisation with ADAM with learning rate 1×10^{-3} for 150,000 iterations.

F. Details and Additional Figures for Section 4.2

F.1. Experimental Details

Data: We consider the dataset from figure 3 with $\mathbf{x} \in \overrightarrow{\mathbf{p}\mathbf{q}}$, where $\mathbf{p} = (-1.2, -1.2)$ and $\mathbf{q} = (1.2, 1.2)$ i.e. the line segment between and including the two data clusters. We evaluate the overconfidence ratio on a discretisation of $\overrightarrow{\mathbf{p}\mathbf{q}}$.

Choosing the Prior: For each depth a fully-connected ReLU network with 50 hidden units per layer is used. The prior mean for all parameters is chosen to be 0. The prior standard deviation for the bias parameters is chosen as $\sigma_b = 1$ for all experiments. In figure 5, the prior weight standard deviation is selected so that the prior standard deviation in function space at the region containing data is approximately constant. In particular, let σ_w/\sqrt{H} be the prior standard deviation of each weight, where H is the number of inputs to the weight matrix. We choose $\sigma_w = \{4, 3, 2.25, 2, 2, 1.9, 1.75, 1.75, 1.7, 1.65\}$ for depths 1-10 respectively, which ensures the prior standard deviations (of both the GP and the BNN) in function space at the points $(1, 1)$ and $(-1, -1)$ (the centres of the data clusters) are between 10 and 15. Choosing a fixed ω such as $\omega = 4$ for all depths would have caused the prior standard deviation in function space to grow unreasonably large with increasing depth; see Schoenholz et al. (2017). All models used a fixed Gaussian likelihood with standard deviation 0.1.

Fitting the GP: The Gaussian process was implemented using GPFlow (Matthews et al., 2017) with the infinite-width ReLU BNN kernel implemented following (Lee et al., 2018). All hyperparameters were fixed and exact inference was performed using Cholesky decomposition.

Fitting MFVI: The weight means in each weight matrix were initialised by sampling from $\mathcal{N}(0, 1/\sqrt{4n_{\text{out}}})$, where n_{out} is the number of outputs of the weight matrix. The weight variances were all initialised to a small value of 1×10^{-5} , following standard best practices for MFVI BNNs (Tomczak et al., 2018). Bias means were initialised to zero. 100,000 iterations of full batch training on the dataset were performed using ADAM with a learning rate of 1×10^{-3} . The ELBO was estimated using 32 Monte Carlo samples during training. The local reparameterisation trick was used (Kingma et al., 2015). The predictive distribution at test time was estimated using 500 samples from the approximate posterior.

Fitting MCDO: The weights were initialised by sampling from $\mathcal{N}(0, 1/\sqrt{4n_{\text{out}}})$, as in MFVI. The biases were initialised to zero. The dropout rate was fixed at $p = 0.05$. The ℓ^2 regularisation parameter was set following Gal (2016, Section 3.2.3) for the given prior, in such a way that the ‘KL condition’ is met, in the interpretation of dropout training as variational inference. 100,000 iterations of full batch training on the dataset were performed using ADAM with a learning rate of 1×10^{-3} . The dropout objective was estimated using 32 Monte Carlo samples during training. The predictive distribution at test time was estimated using 500 samples from the approximate posterior.

Fitting HMC: For HMC on the 1HL BNN, 250,000 samples of HMC were taken using the NUTS implementation in Pyro (Hoffman & Gelman, 2014; Bingham et al., 2018) after 10,000 warmup steps. For the 2HL case, 1,000,000 samples of

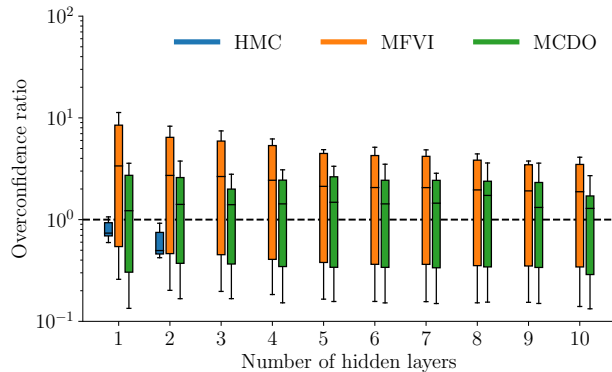


Figure 8. Boxplots of the overconfidence ratios of HMC, MFVI and MCDO relative to exact inference in an infinite width BNN (GP) with $\sigma_w = \sqrt{2}$.

HMC were taken after 20,000 warmup steps. We set the maximum tree depth in NUTS to 5, and adapt the step size and mass matrix during warmup.

F.2. Additional Figures

In order to assess the robustness of our findings to different choices of prior, we also consider the same experiment with $\sigma_w = \sqrt{2}$ for all depths. We choose this prior as it leads to similar variances in function space as depth increases (Schoenholz et al., 2017). We note that the variance of this prior is significantly smaller than the variance of the prior in the previous setting. The corresponding box plot is shown in figure 8. With this prior both methods tend to be less over-confident between data clusters, but more underconfident at the data, especially as depth increases (see figure 9).

G. Initialisation of VI

In order to assess whether the variational objective (ELBO) or optimisation is primarily responsible for the lack of in-between uncertainty when performing MFVI and MCDO, we considered the effect of initialisation on the quality of the posterior obtained after variational inference. In order to find setting of the weights so that the posterior distribution in function space was close to the exact posterior in function space, we initialised the weights of the network by training the network using mean squared loss between the mean and variance functions of a reference posterior and the approximate posterior (as in figure 4). The reference posterior was obtained by fitting the limiting GP with the same priors as the BNN architecture on the dataset (shown in crosses). We used these weights as an initialisation for variational inference. The noise variance was fixed to the true noise variance that generated the data. The data itself was sampled from the limiting GP prior, so that the model should be able to fit the data well.

Two-hidden layer MFVI and MCDO networks were used, with 50 hidden units in both layers. The solution found by minimising squared loss for 50,000 iterations between the mean and variance functions and a reference posterior may lead to distributions over weights such that the KL from these distributions to the prior is high. This can lead to very high values of the variational objective function. To alleviate this behaviour, we gradually interpolate between the squared-error loss and the variational objective, by taking convex combinations of the losses. Call the function space squared loss L_1 and the standard variational objective L_2 . Then after the first 50,000 iterations of using L_1 , we train for 10,000 iterations using $.9L_1 + .1L_2$, 10,000 iterations using $.8L_1 + .2L_2$ and so on until we are only training using L_2 . We then train for 100,000 iterations using just L_2 , to ensure the variational objective has converged. Figure 10 shows that the obtained posterior still lacks in-between uncertainty, providing evidence that this may be due to the objective function rather than overfitting.

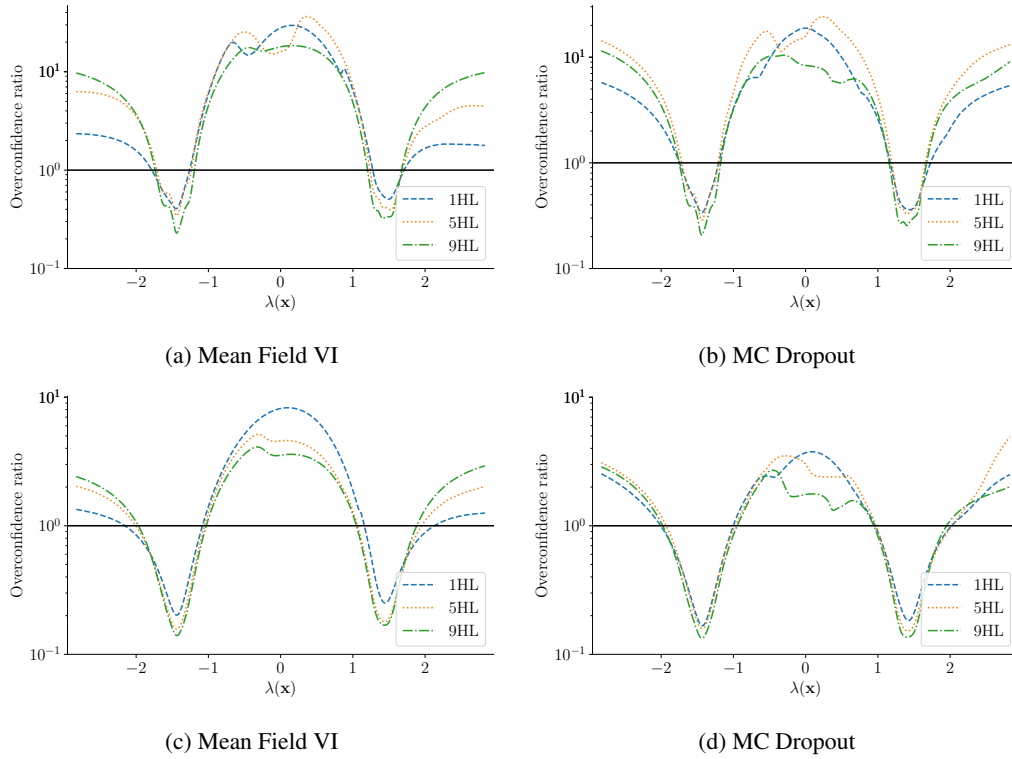


Figure 9. The overconfidence ratio for several depths of neural networks with $\sigma_w = 4, 2, 1.7$ for 1, 5 and 9HL respectively (top), $\sigma_w = \sqrt{2}$ for all depths (bottom) plotted as a function of $\lambda(\mathbf{x})$ (where λ is defined as in figure 3). The data centres are located at roughly $\lambda(\mathbf{x}) = \pm 1.4 \|\mathbb{E}_{q_\phi} [f(X)] - \mu(X)\|_2^2$. We see that both MCDO and MFVI are overconfident in between data, and underconfident at the locations where we have observed data, relative to the GP reference.

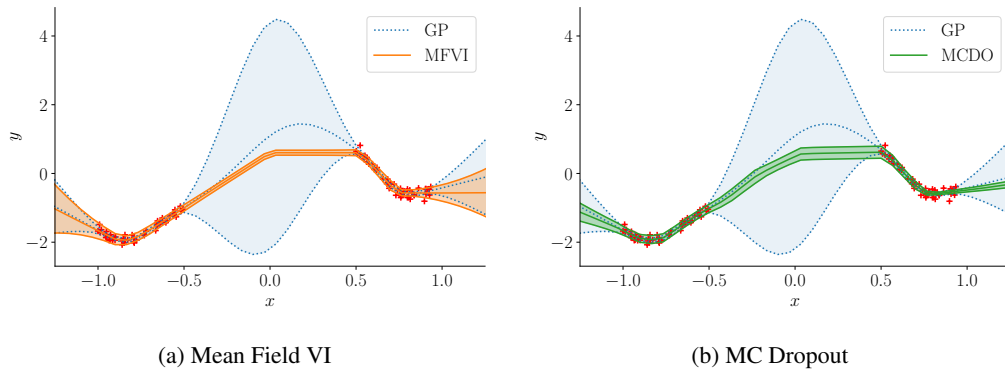


Figure 10. Mean and error bars (± 2 standard deviations) for the GP and the BNN with each inference scheme, trained on the data shown by the red crosses. The inference algorithms were initialised by first minimising the squared error to the reference GP mean and variance, and then running the respective inference algorithm.

H. Details and Additional Plots for Active Learning

H.1. Experimental Setup

As the dataset has low noise, we use a homoskedastic Gaussian noise model with a fixed standard deviation of 0.01 for all models. We used the ADAM optimiser with learning rate 1×10^{-3} for 20,000 epochs to optimise both MFVI and MCDO. We perform full batch training if the active set is smaller than 100 datapoints, otherwise we use a minibatch size of 100. All BNNs are retrained from scratch after the acquisition of each point from the pool set. We used 32 Monte Carlo samples from q_ϕ to estimate the objective function for both MFVI and MCDO. All networks had 50 neurons in each hidden layer. The prior for all BNNs and the GP was chosen to have $\sigma_w = \sqrt{2}, \sigma_b = 1$ (see appendix F for definitions). $\sigma_w = \sqrt{2}$ was chosen so that the prior in function space has a stable variance as depth increases (Schoenholz et al., 2017). The dropout probability was set at $p = 0.05$ for all MCDO networks. The dropout ℓ_2 regularisation was chosen to match the ‘KL condition’ as stated in Gal (2016, Section 3.2.3). The results are averaged over 20 random initialisations and selections of the 5 initial points in the active set. For MFVI and MCDO, the predictive distribution at test time and the predictive variances used for active learning were estimated using 500 samples from the approximate posterior. The parameter initialisations are the same as those in appendix F.

H.2. Additional Figures

Figure 11 shows the points chosen by deep BNNs. Again the GP chooses points from every cluster, and seems to focus on the ‘corners’ of each cluster. MFVI samples from more clusters than the 1HL case, but still comparatively oversamples clusters further from the origin, and undersamples those near the origin. MCDO has a more spread out choice of points than the 1HL case, but still fails to obtain significantly better RMSE than random.

Figures 12 and 13 show the predictive uncertainty of 1HL models at the beginning and end of active learning. All models significantly reduce their uncertainty around clusters that have been heavily sampled, except for MCDO. This causes MCDO to repeatedly sample near locations that have already been labelled, in contrast to the GP. Note also that MFVI is most confident at clusters near the origin that have never been sampled, and least confident at clusters far from the origin that have already been heavily sampled.

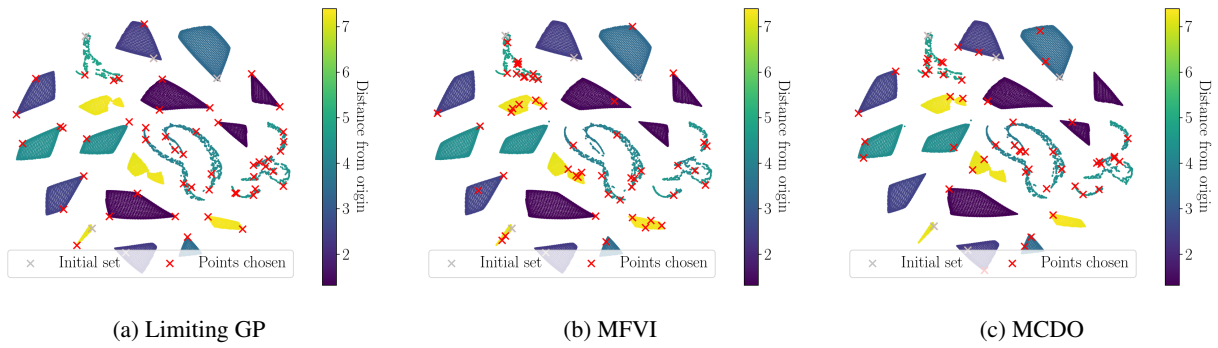


Figure 11. Points chosen during active learning in the 3HL case. Note that t-SNE does not preserve relative positions, so that clusters near the origin may appear on the ‘outside’ of the t-SNE plot.

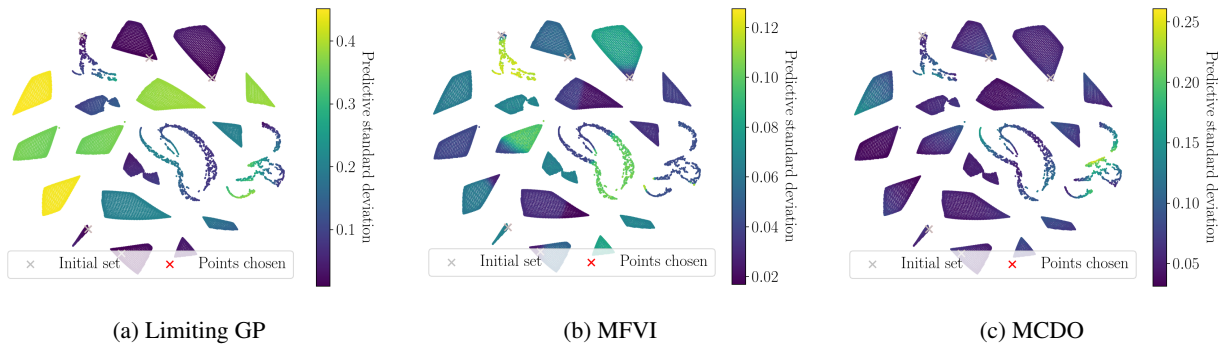


Figure 12. Predictive uncertainties in the 1HL case, at the beginning of active learning. As the noise standard deviation was fixed to 0.01 for all models, changes in the predictive standard deviation reflect model uncertainty.

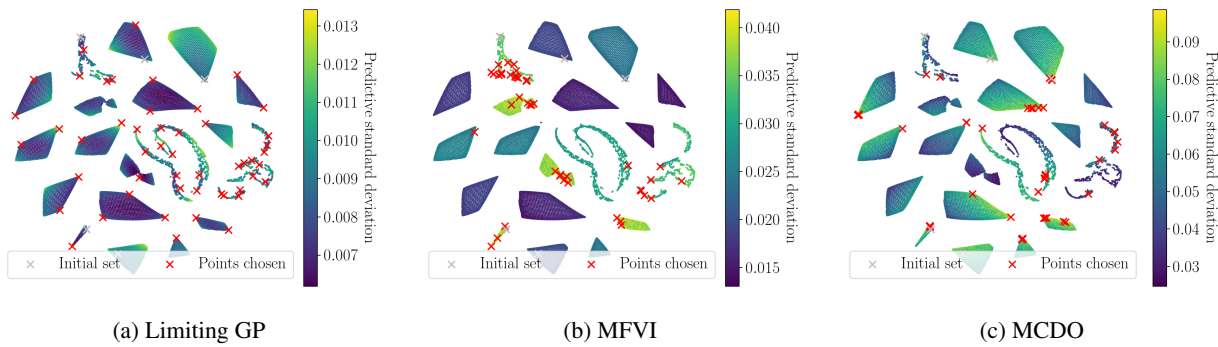


Figure 13. Predictive uncertainties in the 1HL case, after 50 iterations of active learning. As the noise standard deviation was fixed to 0.01 for all models, changes in the predictive standard deviation reflect model uncertainty.